

Catastrophic Bifurcation in the Dynamics of a Threatened Bird Community Triggered by a Planetary-Scale Environmental Perturbation

Pablo Almaraz^{ID*}^{a,b} and Andy J. Green^c

^aDepartamento de Ecuaciones Diferenciales y Análisis Numérico, Facultad de Matemáticas,
Universidad de Sevilla, Campus Reina Mercedes, 41012, Sevilla, Spain.

^bGrupo de Oceanografía de Ecosistemas, Instituto de Ciencias Marinas de Andalucía, CSIC,
Puerto Real, 11519, Spain.

^cDepartamento de Biología de la Conservación y Cambio Global, Estación Biológica de Doñana
EBD-CSIC, Avda. Américo Vespucio 26, 41092, Sevilla, Spain.

*Corresponding Author: Pablo Almaraz. E-mail: pablo.almaraz@csic.es

Abstract

Ecological modeling has been traditionally dominated by a focus on the asymptotic behavior, but transient dynamics can have a profound effect on species and community persistence. We show a strong non-stationary coupling of ecological drivers in one of the world's major Mediterranean ecosystems, Doñana wetlands, which is currently threatened by many stressors. Recurrent changes in precipitation fluctuations triggered sudden reorganizations in community trends and population dynamics of a guild of ten wintering waterfowl species during a 36-year period. An anomalously dry and cold transient period in the Northern Hemisphere induced by the volcanic eruption of Mt. Pinatubo in 1991, prompted an abrupt shift to an alternative regime of fluctuating species densities. Most species did not recover previous values even though local weather patterns and large-scale climatic conditions returned to normal values. Although the dynamical stability of the community is similar in both regimes, structural stability declined: the probability of feasibility dropped across time due to depressed population densities at equilibrium. A stochastic cusp catastrophe model fitted to the time series data suggests that the spatio-temporal persistence of cold and dry conditions in the wintering areas, coupled with warm and wet conditions in the breeding grounds, modulated local ecological conditions and induced hysteresis through behavioral shifts to alternative wintering sites. Our study provides empirical evidence for the existence of a catastrophic bifurcation triggered by a tipping point in the dynamics of an imperiled terrestrial vertebrate community, highlighting the relevance of history and multi-stability in explaining current patterns in biological conservation.

Keywords

Alternative stable states; Doñana wetlands; Stochastic cusp catastrophe; Tipping point; Transient dynamics; Volcanism..

28

Introduction

29 The stability of populations and communities in response to environmental perturba-
30 tions is currently one of the most relevant research topics in the field of global change
31 ecology (Bjornstad 2001; Post 2013; Vellend 2016; Yang et al. 2019). Despite the early
32 appreciation that ecosystems might operate under more than one stable state (e.g.,
33 Holling 1973; May 1977), the main focus of theoretical ecology is still dominated by the
34 asymptotic stability of autonomous (time-independent) ecological models. However, a
35 growing body of evidence suggests that many ecological systems might operate under
36 nonlinear dynamics characterized by abrupt, transient shifts from one stable state to
37 another, usually preceded by tipping points (Fukami and Nakajima 2011; Petraitis 2013;
38 Yletyinen et al. 2016; Rocha et al. 2018; Clements and Ozgul 2018; Dakos et al. 2019;
39 N. Chen et al. 2020). This behavior, commonly known as alternative stable states, is
40 common in marine, freshwater, and terrestrial ecosystems (Steele 1996; Knowlton 2004;
41 Capon et al. 2015; Gsell et al. 2016; review in Rocha, Peterson, and Biggs 2015).

42

43 In global change scenarios, understanding this non-linear behaviour is a major
44 research goal (Rockström et al. 2009; Barnosky et al. 2012; Steffen et al. 2015; Nash
45 et al. 2017). Progress in this field has been largely limited by semantic and statistical
46 confusions on the specific mechanisms, processes and patterns involved in the char-
47 acterization of alternative stable states (Suding, Gross, and Houseman 2004; Capon
48 et al. 2015; Kuiper et al. 2015). A regime shift denotes a statistical change in the pa-
49 rameters forcing a system, while a phase transition alludes to a change in the state of
50 some attribute of the system (Scheffer 2009). From this it follows that regime shifts
51 should usually translate to phase transitions, but the detection of the latter does not
52 necessarily demonstrate the existence of the former (e.g., Rudnick and Davis 2003).
53 Indeed, evaluating whether alternative states are stable is far from trivial (Scheffer
54 2009; Stelzer et al. 2021). Alternative stable states give rise to hysteresis: under the
55 same concurrent environmental conditions there may exist several stable states, and
56 the location of the system in a particular state may be better explained by historical
57 conditions than by present ones (Scheffer 2009; Clements and Ozgul 2018).

58

59 The overall consequence of this is that the abrupt phase transitions detected within
60 ecological time-series are not always explicitly linked to the regime shifts potentially
61 triggering them, thus yielding a rather phenomenological understanding of alternative
62 stable states and regime shifts (Hastings 2004; Montoya, Donohue, and Pimm 2018;
63 Hastings et al. 2018; Hillebrand et al. 2020). Thus, to date it is unclear how abrupt
64 regime shifts at different levels of ecological organization are intertwined, and to what
65 extent this non-linear behaviour stem from external disturbances or internal dynamics

(Scheffer 2009). For example, abrupt ecological disturbances have only recently been linked mechanistically to extreme climatic events, such as large volcanic eruptions and intense hurricanes (e.g., Kuhnt et al. 2005; Schoener and Spiller 2006; Vázquez-Loureiro et al. 2019; Osland et al. 2020). In particular, volcanism is regarded as one of the major perturbations not only to planetary climate (Osipov et al. 2021; Millán et al. 2022), but also to ecological systems at all organizational, temporal and spatial scales (Sadler and Grattan 1999; Oppenheimer 2003; Crisafulli et al. 2015; Jiang et al. 2022; Green, Renne, and Keller 2022; Z.-Q. Chen et al. 2022; Cabon and Anderegg 2022). One of the most recent major volcanic eruptions was that of the Mount Pinatubo on Luzon Island, Philippines, in 1991. This eruption is classified by geologist as a colossal event, with a return time between 50 and 100 years (e.g., Labitzke and McCormick 1992; Robock 2000). After producing the largest stratospheric volcanic aerosol cloud of the 20th century, the climatic impacts of Mt. Pinatubo eruption were of a planetary scale and lasted for several years (McCormick, Thomason, and Trepte 1995; Robock 2002; Douglass and Knox 2005). The Mt. Pinatubo eruption provided a natural experiment testing the response of the global atmosphere and biosphere to large geological phenomena (Soden et al. 2002; Church, White, and Arblaster 2005; Khodri et al. 2017; Booth et al. 2012). Consequently, a suite of ecological effects of this transient major perturbation were detected in several world ecosystems (Genin, Lazar, and Brenner 1995; Lucht et al. 2002; Gu et al. 2003; Kuhnt et al. 2005; Trenberth and Dai 2007). Nevertheless, by definition, the frequency of such events is rare, so there are few opportunities to study the effects of single major perturbations on ecological dynamics in the long-term, while accounting for system dynamics before and after the perturbation.

Using a 36-year (1978–2013) dataset of abundance fluctuations of a wintering waterfowl community, we provide evidence on the coupling of abrupt shifts in the environmental, anthropogenic and biological subcomponents in one of the largest and best preserved Mediterranean wetland ecosystems in the world (Doñana wetlands, SW Spain; Rendón et al. 2008; Almaraz et al. 2012; Green et al. 2018). This major ecosystem, historically supporting more than 1 million wintering birds from breeding grounds across the Palaearctic, is a Biosphere Reserve and includes a UNESCO World Heritage site. In spite of this, it is currently considered under severe threat due to several anthropogenic stressors, mainly groundwater abstractions and greenhouse-based agriculture (Scheffer et al. 2015; Green et al. 2017; Green et al. 2018; Camacho et al. 2022; Santa-maría and Martin-Ortega 2023; Felipe, Aragonés, and Díaz-Paniagua 2023). Waterbird communities are particularly useful for time-series analysis, because their populations are relatively easy to count, and can act as useful bioindicators of wetland biodiversity (Green and Elmberg 2014). Previous analyses (Almaraz et al. 2012) detected an abrupt shift in the wintering waterfowl community of Doñana wetlands synchronized with a

105 climatically harsh period lasting from 1992 to 1995. This low population density regime
106 apparently became permanent even though local weather conditions returned to normal
107 values. This transient period, characterized by anomalously dry and cold wintering
108 seasons, is linked to the injection of massive amounts of sulfate aerosols by the eruption
109 of Mt. Pinatubo (Robock 2002; Soden et al. 2002; Booth et al. 2012). These conditions
110 persisted several years across the southern Palaearctic, with a reversed climatology
111 in the northern Palaearctic characterized by warm and wet wintering seasons. Our
112 main hypothesis is that the persistent anomalous conditions throughout the Palaearctic
113 linked to Mt. Pinatubo eruption triggered a bifurcation between alternative stable states
114 in the dynamics of the migratory wintering waterfowl of Doñana wetlands. Some
115 evidence indicates that the drop in wintering waterfowl numbers in Doñana wetlands
116 was synchronized with abrupt changes in the breeding and wintering populations of
117 waterbirds communities across the Western Palaearctic (Ganter and Boyd 2000; Mitchell
118 et al. 2008; Christensen and Fox 2014), and these changes were already hypothesized to
119 be linked to the eruption of Mt. Pinatubo.

120

121 Here we suggest that the cold and dry wintering conditions in our study area during
122 the transient anomalous period translated to persistent behavioral shifts in site selec-
123 tion and migratory behaviour of waterfowl. Decision-making by individuals of social
124 species can propagate to the population and community levels through well-known
125 runaway mechanisms, such as social copying (Oro 2020; Oro et al. 2023). For example,
126 environmental perturbations can induce highly complex ecological dynamics by linking
127 individual decisions with permanent shifts in the fidelity to wintering or stopover sites
128 and flyway routes of migratory animals (Almaraz and Oro 2011; Almaraz et al. 2012;
129 Oro 2020; Oro et al. 2023; Piersma and Gils 2011). In waterfowl, winter philopatry is
130 generally low due to highly plastic behaviour at the individual and population scales in
131 response to weather fluctuations (Robertson and Cooke 1999; Adam et al. 2015; Clausen
132 et al. 2018; Fox et al. 2023). Since there is a genetic, female-biased component to site
133 fidelity, it can be hypothesized that long-lasting harsh conditions on the wintering
134 grounds may prompt permanent shifts to alternative wintering sites and migration
135 routes. We test this specific hypothesis using a suite of modeling approaches. First,
136 we use Bayesian Dynamic Factor analysis and Hidden Markov Models (Almaraz and
137 Oro 2011; Ward et al. 2022) to test for the existence of abrupt shifts and persistent
138 alternative regimes in species- and community-level densities across time. Secondly,
139 we fit a regime-dependent extension of a multivariate state-space model (Almaraz
140 et al. 2012) to check for the existence of alternative stable states and shifting feasibility
141 properties of the wintering community across different density regimes. Finally, we
142 apply a stochastic cusp catastrophe model (Cobb and Zacks 1985) to test for the specific
143 hypothesis that the existence of regime shifts and alternative stable states is linked to

144 the press-type perturbation of the Mt. Pinatubo eruption of planetary climate. From a
145 conservation standpoint, the major implication would be that characterizing the history
146 of an ecosystem is of paramount importance when management actions are directed at
147 specific stressors that may not be currently operating (Scheffer 2009; Scheffer et al. 2015).

148

149 Material and Methods

150 Study area, environmental data and bird community time series

151 The Doñana wetlands are located in South-western Spain, and are composed of a com-
152 plex mosaic of natural wetland ecosystems and artificial salt pans, ricefields, and fish
153 farms within the large (>150.000 Ha) inner delta of the Guadalquivir river (Rendón
154 et al. 2008; Almaraz et al. 2012; Green et al. 2018). This area is one of the best preserved
155 Mediterranean wetland ecosystems in the world, and is one of the major wintering and
156 stopover sites for waterbirds breeding throughout the Western Palaearctic. However, it
157 is currently under threat from increases in water extraction and eutrophication from
158 agricultural intensification, as well as from climate change (Marín and García 2006;
159 Scheffer et al. 2015; Green et al. 2017; Camacho et al. 2022). A total of circa. 100 000 ha
160 have been surveyed from the air on a monthly basis by the same three expert observers
161 since 1973, providing total counts of the 10 most abundant wintering waterfowl (Anati-
162 dae) species: the Pintail (*Anas acuta*), Shoveler (*Spatula clypeata*), Common Teal (*Anas*
163 *crecca*), Eurasian Wigeon (*Mareca penelope*), Mallard (*Anas platyrhynchos*), Gadwall (*Mareca*
164 *strepera*), graylag goose (*Anser anser*), Common Pochard (*Aythya ferina*), Red-crested
165 pochard (*Netta rufina*), and Shelduck (*Tadorna tadorna*) (see Rendón et al. 2008 for count-
166 ing methods). Complete data exist for every species from 1978 until nowadays. We used
167 two estimated population sizes for each waterfowl species every year (December and
168 January), and control for observation error through a state-space approach (Almaraz
169 et al. 2012; see **Estimating community stability and feasibility** section below). The win-
170 tering population size ranged from a minimum of 61.282 birds to a maximum of 534.460.

171

172 The size of the waterfowl population depends strongly on the amount of flooded
173 surface in the natural marsh and in artificial habitats. The extension of ricefields depend
174 on rainfall during previous winters, and not on the flooded area of the marsh, since
175 their hydrology is different (Green et al. 2018). Therefore, in a given year of low rainfall,
176 the natural marsh can be dry but the rice cover can still be high (Ramo et al. 2013; Rees
177 et al. 2021). The fish ponds and salt pans are permanently flooded, and their surface
178 area was expanded during the study period (Rendón et al. 2008; Walton et al. 2015.
179 Different wetland types support different communities, and the natural marshes are

180 specially important for ducks and geese (Rendón et al. 2008; Sebastián-González and
181 Green 2016). To assess the potential coupling between phase transitions in waterfowl
182 populations and environmental dynamics, we used annual figures for the extension
183 of winter flooding in the surveyed area, obtained from satellite imagery and averaged
184 from November to February, for the surface covered with cultivated ricefields each
185 year (see Almaraz et al. 2012 for details). Finally, we used monthly precipitation and
186 temperature time-series gathered within Doñana National Park from 1978 onwards.
187 We explored the structure of fluctuations in the precipitation time-series by extending
188 the temporal analysis to the frequency domain through wavelet analysis (Torrence and
189 Compo 1998; Cazelles et al. 2008).

190

191 Climatic and volcanic database

192 We constructed a synoptic climatology of the western Palaearctic, including both
193 the breeding and wintering grounds of the ten waterfowl species considered, for
194 the studied time period and during all seasons except summer. This included the
195 region from 30N to 80N, and from 20W to 45E (Fig. 2). We extracted time-series
196 data from the Version 3 (V3) of The Twentieth Century Reanalysis Project (https://psl.noaa.gov/data/20thC_Rean/), developed by the Physical Sciences Laboratory
197 of the National Oceanographic and Atmospheric Administration. We reconstructed
198 the fields for air temperature and precipitation rate, and produced plots of composite
199 anomalies for both variables: as suggested by the SDC and wavelet analyses, a transient
200 dry and cold period was detected from 1992 to 1995. We thus compared the composite
201 anomalies for air temperature and precipitation rate from 1978 to 2013 (excluding the
202 transient period 1992-1995), with the composite anomalies of the transient period (1992-
203 1995).

204

205 Several indices are available for characterizing the magnitude of volcanic eruptions
206 (e.g., Crosweller et al. 2012; Constantinescu et al. 2021). The multi-decadal variability
207 in the North Atlantic climate is under strong forcing by stratospheric aerosols (Otterå
208 et al. 2010; Booth et al. 2012; Knudsen et al. 2014). Volcanic activity is one of the main
209 natural sources of aerosols to the stratosphere (Otterå et al. 2010; Constantinescu et
210 al. 2021), so an index of Volcanic aerosol optical depth of the stratosphere (SAOD, Booth
211 et al. 2012) has been suggested as a surrogate for evaluating the impacts of Volcanic
212 activity on global climate through the forcing of the upper atmosphere. We used the
213 monthly AOD index for the Northern Hemisphere (35.2 °N and 58.7 °N) from Booth
214 et al. 2012 as a surrogate for climatic forcing of volcanic activity in the breeding and
215 wintering areas of Palaearctic waterfowl (See Fig. 1).

217

218

Detecting community trends and regime shifts

219 We used Bayesian state-space Dynamic Factor Analysis (DFA; Almaraz and Oro 2011;
 220 Ward et al. 2022) to detect and characterize major trends, and potentially regime shifts,
 221 in the long-term wintering time-series of the waterfowl community. A DFA is a mul-
 222 tivariate dimension-reduction technique analogous to Factor Analysis, and its main
 223 goal is to extract the major temporal trends in abundance of the community emerging
 224 from the simultaneous trend of each species, while accounting for observation error
 225 (see Ward et al. 2022 for an introduction). It is thus a sort of joint species model where
 226 the output is a suite of modeled community trends (factors) and a collection of factor
 227 loadings representing the regression of each single-species temporal trend on every
 228 common trend. A state-space DFA model has two equations: a (latent) process, or state
 229 equation; and an observation or measurement model linking the state process to the
 230 observations. The DFA can be written as:

$$\begin{aligned} \mathbf{x}_{t+1} &= \mathbf{S}(\mathbf{x}_t) + \mathbf{w}_t \\ \mathbf{y}_t &= \mathbf{Z}\mathbf{x}_t + \mathbf{e}_t \end{aligned} \tag{1}$$

231 were \mathbf{x} is an $T \times K$ matrix of K latent trends (dynamic factors) and T years. The term
 232 $\mathbf{S}(\mathbf{x}_t)$ represents smoothed functions capturing the autoregressive evolution of the
 233 latent trends. These functions are constructed using P- or B-splines, Gaussian Predictive
 234 Processes, or random walks (Ward et al. 2022). The process error of the latent trends
 235 equation, \mathbf{w}_t , follows a multivariate normal distribution, $\mathbf{w}_t \sim \mathcal{MVN}(0, \mathbf{Q})$ where \mathbf{Q}
 236 is generally assumed to be a $T \times K$ positive semi-definite matrix. The trends \mathbf{x}_t are
 237 linked to the observations \mathbf{y}_t , the wintering waterfowl counts of each species through
 238 the observation or measurement model. We stress that we are using two counts each
 239 winter, replicated in December and January each year, for each species, so that the DFA
 240 is fully identified (see Almaraz and Oro 2011; Almaraz et al. 2012; Ward et al. 2022). In
 241 this case, \mathbf{Z} is a matrix of estimated factor loadings, dimensioned as $P \times K$, were P is
 242 the number of time series. Again, the residual observation errors are assumed to be
 243 multivariate normally distributed, $\mathbf{e}_t \sim \mathcal{MVN}(0, \mathbf{R})$, where R is generally assumed to
 244 be a $T \times K$ positive semi-definite matrix.

245 We used flexible P-Spline functions for constructing the terms \mathbf{S} (Eilers and Marx
 246 1996; Ward et al. 2022). We fitted a DFA with two common trends ($K = 2$), and each
 247 P-Spline was fitted with 16 knots; this is the value that minimizes the score from leave-
 248 on-out cross-validation (see Ward et al. 2022). Since we implemented the DFA with
 249 two replicated wintering counts each year, the model explicitly accounted for variable

observation errors among years (see Ward et al. 2022). After estimating the common trends, we used a Hidden Markov Model (HMM, Fraser 2008) with two regimes to detect and localize potential regime shifts in the common trends. HMMs were fitted to the two major trends. We fit the DFA in Eqn. 1 with the R package bayesdfa (Ward et al. 2022), which implements the Hamiltonian Monte Carlo NUTS algorithm of the Stan probabilistic programming language (Carpenter et al. 2017).

256

257 Modeling community dynamics

After characterizing the existence and location of the regime shift, we fitted a state-space Lotka-Volterra-Ricker (LVR) model to each of the regimes to evaluate their relative stability and feasibility properties (Almaraz and Oro 2011; Almaraz et al. 2012; Mutshinda, O'Hara, and Woiwod 2011). We denote the first regime identified by the DFA in the dominant common trend, or dynamic factor (Fig. 3) with the subscript 1 for each of the parameters, and the second regime with the subscript 2. The LVR regime-dependent state-space model can be written as:

$$n_{i,t+1} = \begin{cases} n_{i,t} + r_{1,i} \left(1 - \frac{\sum_{j=1}^s \alpha_{1,ij} N_{j,t}}{K_{1,i}} \right) + \gamma_{1,i} F_t + \epsilon_{1,i,t} & \text{for } 1978 < t < 1992 \\ n_{i,t} + r_{2,i} \left(1 - \frac{\sum_{j=1}^s \alpha_{2,ij} N_{j,t}}{K_{2,i}} \right) + \gamma_{2,i} F_t + \epsilon_{2,i,t} & \text{for } 1995 < t < 2013 \end{cases} \quad (2)$$

$$n_{i,0} = \begin{cases} \mu_{1,i,0} + \epsilon_{1,i,0} & \text{for } 1978 < t < 1992 \\ \mu_{2,i,0} + \epsilon_{2,i,0} & \text{for } 1995 < t < 2013 \end{cases} \quad (3)$$

$$y_{i,k,t} = \begin{cases} n_{i,t} + b_{1,i,k} + \tau_{1,t,i} & \text{for } 1978 < t < 1992 \\ n_{i,t} + b_{2,i,k} + \tau_{2,t,i} & \text{for } 1995 < t < 2013 \end{cases} \quad (4)$$

where $n_{i,t}$ is the \log_e population abundance of each waterfowl species i during each winter, and $N_{i,t}$ is the raw population abundance. Omitting the subscripts for each regime for the sake of clarity, the per-capita (intrinsic) growth rates of each waterfowl species is denoted by r_i . The interaction matrix \mathbf{A} is formed by the coefficients of inter-specific interactions scaled by the carrying capacities of each waterfowl species in the off-diagonal, α_{ij}/k_i . The intra-specific coefficients in the diagonal, α_{ii} , are k_i^{-1} (see Ranta, Lundberg, and Kaitala 2006; Mutshinda, O'Hara, and Woiwod 2009; Almaraz and Oro 2011). We regularized the interaction matrix through spike-and-slab priors on the coefficients of inter-specific interactions (see Almaraz et al. 2012 and the Supplementary Material). The parameters γ_i measure the impact of flooding extension, F_t on species-level population growth-rate during each regime.

276

277 The terms $\epsilon_{i,t}$ represent the impact of process stochasticity on the abundance of
 278 each species, with variance σ_i^2 . These terms fill the diagonal of the matrix Σ in the
 279 state equation: the diagonal of this matrix thus includes the variance of the unmod-
 280 elled (stochastic) environmental factors impacting on single-species dynamics, while
 281 the off-diagonal contains the (potentially) co-varying joint responses to the common
 282 environment among all species, $cov(\sigma_i, \sigma_j)$. This matrix is, thus, positive semi-definite
 283 and symmetric (Almaraz and Oro 2011; Almaraz et al. 2012). The initial state, $n_{i,0}$ for
 284 each waterfowl species in the vector of latent states is specified as a normal distribution
 285 with mean μ_{i,n_0} and variance $\sigma_{n_0}^2$, $n_{i,0} \sim \mathcal{N}(\mu_{i,0}, \sigma_{n_0}^2)$.

286

287 Finally, the latent population abundances in Eqn. 2 are linked through the obser-
 288 vation equations, eqn. 4, to the observed abundances in the aerial censuses, $\mathbf{y}_{i,t}$. The
 289 observations contains two k values for each species i and winter t : one for December
 290 and the other for January ($y_{i,k,t}$ were k is the month). The column vectors \mathbf{b}_k include
 291 the correction factors for the average fluctuation level of each wintering census (i.e. the
 292 difference between December and January counts) and for each waterfowl species. The
 293 correction factors for the December replicate were set to 0, while the other parameters
 294 were estimated freely. This allowed for identifiability (Mutshinda, O'Hara, and Woiwod
 295 2011; Almaraz et al. 2012). The terms $\tau_{t,i}$ stand for the impact of measurement error
 296 on latent state estimation for each species, with observation variance ρ_i^2 . Again, these
 297 measurement variances fill the diagonal of the matrix Ω , and we also modeled the
 298 potentially co-varying observation error between species in the off-diagonal terms:
 299 $cov(\rho_i, \rho_j)$.

300

301 We used Bayesian Markov Chain Monte Carlo (MCMC) through Gibbs sampling
 302 to fit the regime-dependent state-space LVR model (Eqns. 2-4) to the waterfowl com-
 303 munity time series (see Almaraz et al. 2012; Mutshinda, O'Hara, and Woiwod 2011).
 304 The models were written in the JAGS probabilistic programming language (Plummer
 305 2003), interfaced with the runjags package in R (Denwood 2016). We ran three parallel
 306 chains for 130.000 iterations, discarding the first 100.000 as burn-in. We used the pack-
 307 age ggmc (Fernández-Marín 2016) for diagnosing the convergence on the posterior
 308 distribution.

309

310 Estimating community stability and feasibility

311 To evaluate the stability of the equilibrium for each community abundance regime
 312 detected by the DFA, we constructed the Jacobian matrix of the LVR model (e.g., Ranta,

³¹³ Lundberg, and Kaitala 2006); for simplicity, we omit the subscript for each regime, but
³¹⁴ we recall that there are two Jacobians. In the LVR discrete-time model the equilibrium
³¹⁵ abundance vector, \mathbf{N}^* , is given by $\mathbf{N}^* = \mathbf{A}^{-1}\mathbf{K}$. The Jacobian matrix is then written as:

$$\mathbf{J} = \begin{pmatrix} 1 - \frac{r_1}{k_1} N_1^* & \cdots & -\frac{\alpha_{1s} r_1}{k_1} N_1^* \\ \vdots & \ddots & \vdots \\ -\frac{\alpha_{s1} r_s}{k_s} N_s^* & \cdots & 1 - \frac{r_s}{k_s} N_s^* \end{pmatrix} \quad (5)$$

³¹⁶ The criteria for the dynamical stability of a discrete-time system is that the spectral
³¹⁷ radius of the Jacobian should be strictly less than 1 (Elaydi 2005), so we tested if the
³¹⁸ modulus of the dominant eigenvalue of matrix \mathbf{J} (5) is contained within the unit circle in
³¹⁹ the complex plane during the different regime shifts detected (see Results). We thus de-
³²⁰ fine the probability of dynamical stability as the frequency of spectral radii of the matrix
³²¹ \mathbf{J} (5) that were < 1 in the posterior distribution. If this condition is fulfilled during the
³²² distinct regimes detected, this provides evidence of the existence of alternative stable
³²³ states. Further, we estimated the posterior asymptotic resilience of each distinct regime
³²⁴ as the inverse of the maximum absolute real part of the eigenvalue spectra (Arnoldi,
³²⁵ Loreau, and Haegeman 2016).

³²⁶

³²⁷ Dynamical stability measures the asymptotic behavior of small perturbations of
³²⁸ the state variables of a linearized system in the vicinity of an equilibria. In contrast,
³²⁹ structural stability quantifies whole-system responses: the range of perturbations of
³³⁰ parameters of a dynamical system that produce the same qualitative dynamics (Thom
³³¹ 1977; Almaraz et al. 2023). In ecology, a useful criteria for assessing structural stability
³³² is the characterization of the feasibility domain (Logofet 1993; Roberts 1974): the range
³³³ of the environmental conditions yielding an equilibrium where all species have positive
³³⁴ abundances (Song and Saavedra 2018). In our case, this would imply that the poste-
³³⁵ rior distribution of the equilibrium abundance vector \mathbf{N}^* should contain only positive
³³⁶ values. Therefore, taking advantage of the effective propagation of uncertainty of the
³³⁷ Bayesian state-space approach, we define here the empirical probability of feasibility
³³⁸ as the fraction of strictly positive posterior samples of \mathbf{N}^* . Changes in this probability
³³⁹ between alternative stable states would indicate shifts in the structural stability of the
³⁴⁰ modeled system. That is, even though dynamical stability is conserved, structural sta-
³⁴¹ bility could change as a consequence of changing impacts of environmental conditions
³⁴² on the size of parameter space compatible with a feasible community.

³⁴³

344

Stochastic cusp catastrophe modeling

345 Finally, we applied stochastic catastrophe theory (Cobb and Zacks 1985; Grasman, Maas,
 346 and Wagenmakers 2009) to model the links between the global climatic transient forcing
 347 induced by the Mt. Pinatubo eruption on the regime shifts in the wintering waterfowl
 348 community. We hypothesize that this link operates through the press perturbation of
 349 the large-scale weather conditions in the full distribution area of the studied water-
 350 fowl species, namely the Western Palaearctic. This press perturbation reorganized the
 351 wintering populations at a continental scale, with potentially long-lasting shifts in the
 352 migratory behavior.

353

354 As a branch of nonlinear dynamical systems and bifurcation theory, catastrophe
 355 theory, originally developed by René Thom (Thom 1975, 1977), has seen some appli-
 356 cations in marine sciences over the last decades. For example, catastrophic dynamics
 357 has been recently suggested as an explanation for the collapse of Atlantic Cod (*Gadus*
 358 *morhua*) fisheries during the last decades (Sguotti et al. 2019). The perspective provided
 359 by catastrophe theory is particularly relevant for systems characterized by sudden shifts
 360 between alternative stable states induced by smooth changes in control parameters
 361 (Casti 1982; Loehle 1989). In the Supplementary Material we describe in detail the
 362 rationale behind catastrophe theory. In brief, our phenomenological hypothesis (Eqn.
 363 6) is that the smooth temporal changes in the impact of the spatial flooding extension
 364 can become nonlinear and discontinuous, and trigger regime shifts to alternative stable
 365 states in the major community trend of the DFA, under the forcing of Volcanic-induced
 366 shifts in planetary climate fluctuations. Namely, volcanic forcing, as measured through
 367 the stratospheric aerosol optical depth (Booth et al. 2012) operates as a bifurcation pa-
 368 rameter (β -parameter, (Grasman, Maas, and Wagenmakers 2009)), forcing the system to
 369 go through a catastrophic bifurcation between alternative stable states that share a range
 370 of environmental conditions. In contrast, flooding extension is an asymmetry parameter
 371 (α -parameter), measuring the skew in the distribution of alternative states across this
 372 range of environmental conditions. This is indeed the region of hysteresis, where history
 373 is important: where the system comes from is crucial to evaluate why it is now in the
 374 state it is, and how can it be pushed to a desired state through, e.g., management actions
 375 (Petraitis 2013; Scheffer 2009; Scheffer et al. 2015). The cusp catastrophe model would
 376 take the form:

377

$$\begin{aligned}\alpha &= \alpha_1 F \\ \beta &= \beta_0 + \beta_1 SAOD \\ y &= \omega_0 + \omega_1 x_1\end{aligned}\tag{6}$$

378 where, as noted, α and β are the asymmetry and bifurcation parameters, respectively,
379 that are modeled as canonical variables (Grasman, Maas, and Wagenmakers 2009).
380 These variables are smooth transformations of the control variables F (flooding exten-
381 sion) and $SAOD$ (stratospheric aerosol optical depth). The canonical variable y is the
382 state of the system, here represented by the major community trend detected by the
383 DFA, x_1 .

384 We used the R package `cusp` to fit the cusp catastrophe model (Grasman, Maas,
385 and Wagenmakers 2009). The cusp equilibrium surface, and the coefficients of the
386 smooth transformation in Eqn.s 6, $\alpha_1, \beta_0, \beta_1, \omega_0, \omega_1$, were obtained through maximum-
387 likelihood methods. The fitting of a linear and a non-linear (logistic) model was com-
388 pared with the cusp catastrophe using information criteria and $pseudo - R^2$. Further
389 details are given in Supplementary Material.

390

391 Results

392 Weather and climate fluctuations

393 Figure 1 shows the fluctuations in the stratospheric optical depth in the northern
394 hemisphere, temperature, precipitation and spatial flooding extension of the study
395 area from 1978 to 2013. While seasonality in the signal for temperature is strong and
396 was never lost, precipitation did exhibit a more irregular pattern. The wavelet power
397 spectrum is shown for precipitation (1E): the 1991-1995 period stand out as particularly
398 irregular . Finally, the volcanic aerosol optical depth shows two salient peaks coinciding
399 with the two largest volcanic eruptions of the study period (1A). The inset figure shows
400 the standardized values for precipitation, temperature and flooding for volcanic vs.
401 non-volcanic years. During volcanic years, the local weather was significantly cooler
402 and drier, and the extension of the flooded area was therefore smaller.

403 The synoptic fields of composite anomalies for 1978 to 2013 obtained from the Twen-
404 tieth Century Reanalysis Project (Fig. 2) reveal a clearly temporal and spatial divergent
405 pattern at a continental scale: the reconstructed anomalies for temperature and precipi-
406 tation rate for the period of transient climatic perturbation of the Mt. Pinatubo eruption
407 (1991-1995) shows a particularly dry and cold period for southern Europe and northern
408 Africa and a relatively warm and wet period for the northern Palaearctic (Fig. 2B, D).
409 When excluding these years, this pattern is reversed: a relatively warm and wet period
410 characterized winters in the southern Palaearctic (Fig. 2A, C).

411

412 Major trends in the community

413 The major waterfowl community trends modeled by the state-space Dynamic Factor
414 Analysis (DFA) are shown in Figure 3. A first trend displayed a clear abrupt shift in 1992
415 towards significantly lower levels, a shift that was sustained through time. In contrast, a
416 second trend displayed a downward peak around 1992, and a further increase through
417 time. A DFA with only one trend is a worse model relative to a two-trend model
418 according to the leave-one-out cross-validation information criterion (ΔLOOC : 53.872).
419 Indeed, the Hidden Markov Model (HMM) of regime shifts, when applied to the first
420 trend (Trend 1 in Fig. 3), suggested a highly significant shift in 1992. A HMM with
421 no regime shift is a much worst predictor than a HMM with at least one regime shift
422 (ΔLOOC : 114.126). The fitting of the species-specific dominant trends to each time
423 series is shown in Figure 4, with associated loading factors in Figure 5. The magnitude
424 of the abrupt shift in 1992 differed somewhat among species, and is particularly strong
425 for some, such as the Common Teal, the Eurasian Wigeon, the Gadwall, the Shelduck
426 and the Graylag Goose. Overall, the DFA analysis suggests that the abrupt shift in 1992
427 is a generalized dynamic shift across the community, with weak, subsequent recoveries
428 only for some species.

429

430 Characterizing alternative stable states

431 According to the community regime shift detected by the DFA in 1992, and the transient
432 period towards the second fluctuation level, that started in 1995 (Fig. 3, 4), the state-
433 space LVR model was fitted to two separate periods: from 1978 to 1992; and from
434 1995 to 2013 (see Eqns. 2-4). The posterior quality checking of model fitting suggests
435 that MCMC chains mixed well and showed evidence of convergence in both periods.
436 Additionally, posterior predictive checks suggest that the fitted Bayesian state-space
437 LVR model is able to reproduce closely the original time series for both regimes (see
438 Supplementary Material). The impact of flooding extension on the growth-rate of the
439 waterfowl species is generally positive for all species in both dynamic regimes. The
440 probability of inter-specific interaction, as selected by the regularization scheme (see
441 Supplementary Material), was very low in both periods (less than 0.04). Interestingly,
442 the posterior probability of dynamic stability and resilience are similar for both periods
443 (Figure 6A, B). While the posterior distribution of the dominant eigenvalues of the
444 Jacobian are close to 1 in both periods, the linearized dynamics around the equilibrium
445 are stable with a very large probability. This is strong evidence of alternative stable
446 states.

447 The probability of feasibility, measured as the fraction of posterior equilibrium abun-
448 dance vectors with strictly positive values, dropped from 0.992 before the Mt. Pinatubo

eruption to 0.634 after the event (Figure 6C, D). Although the probability of extinction was low for all waterfowl species, in all cases this probability increased in the second alternative stable state after the Mt. Pinatubo eruption (Fig. 7), particularly for the Gadwall. Overall, while dynamical stability does not change among regimes, structural stability drops after the explosion of Mt. Pinatubo.

454

455 Cusp catastrophe modeling

456 The results of the fitting of the cusp catastrophe modeling to the major community trend
457 are shown in Table 1. The cusp model (Eqn. 6) is clearly the best one for explaining
458 the observed pattern of covariation of the major community trend, the volcanic aerosol
459 stratospheric optical depth (SAOD) and spatial flooding extension. This model accounts
460 for the 95.4% of variance of the major DFA trend displaying a regime shift (Trend 1 in
461 Fig. 3). The maximum-likelihood estimates, and their associated uncertainty, of the
462 parameter of the cusp catastrophe model (Eqn. 6) are shown in the Supplementary
463 Material.

464 The diagnostic plot for the fitted cusp catastrophe model (see Supplementary Mate-
465 rial) suggests that all values are located in the region of the bifurcation set, providing
466 strong evidence for the presence of a catastrophic bifurcation between alternative stable
467 states. A 3D plot of the cusp catastrophe model (Fig. 8B) verifies that the waterfowl
468 community fluctuated during the full 36 year period in the region of multi-stability.
469 This is more clearly assessed in the transition plot of the major community trend (Fig.
470 8C): two fluctuating regimes, clearly separated by an abrupt transition in 1992 after Mt.
471 Pinatubo eruption (Fig. 8A), indicate a fundamental regime shift between alternative
472 stable states after a tipping point in 1992. The hysteresis region covers all the fluctuating
473 range of flooding extension.

474

475 Discussion

476 Our results provide an empirical example of a catastrophic bifurcation after a tipping
477 point in a major threatened biodiversity hotspot induced by an abrupt geological dis-
478 ruption with global impacts on the atmosphere, the biosphere and the ocean. We have
479 found a persistent regime shift between two alternative stable states in the wintering
480 dynamics of a vertebrate guild of one of the world's most iconic wetland ecosystems
481 (Scheffer et al. 2015) over a 36 year study period. As examples of abrupt shifts in
482 birds, Durant et al. 2004 showed the existence of regime shifts in breeding parameters
483 of a seabird linked to oceanographic changes in the Norwegian Sea, and Jenouvrier

et al. 2005 found discrete shifts in the cycling dynamics of three seabirds breeding in the Antarctic, correlated with changes in the climatic conditions of the Southern Ocean. In the present paper, a detailed pattern of covariation between external forcing variables and the fluctuations of a wintering waterfowl community conform very well to a cusp catastrophe, where the ecological dynamics depend not only on the local environmental conditions, but also on the external, large-scale forcing climatic conditions modulating the transition from a smooth, linear system behaviour to a discontinuous, nonlinear dynamics. Indeed, the modeled shift has been statistically linked to an abrupt perturbation of planetary climate for which a detailed forcing mechanism has been identified, namely the eruption of Mt. Pinatubo, Philippines, in June 1991 (Hansen et al. 1992; Labitzke and McCormick 1992; Robock 2000, 2002; Douglass and Knox 2005). A general, transient (2-4 years) worldwide cooling of the troposphere, inducing cold summers and warm winters in the Northern Hemisphere and a transient reversal of the global warming trend (Robock 2000, 2002; Lucht et al. 2002; Church, White, and Arblaster 2005; Smith et al. 2016), points to the Mt. Pinatubo eruption, with more than 20 megatons of SO_2 injected into the stratosphere (Hansen et al. 1992), as the single most important geological event of the 20th century. The transient pattern of cooling in southern Europe and warming of Northern Europe immediately after the eruption was reproduced in this study, with evidence that this led to long-lasting shifts in the behaviour of migratory birds. Several biological signals have already been linked to the Mt. Pinatubo eruption, such as the remote control of net primary production (Lucht et al. 2002; Krakauer and Randerson 2003), shifts in deep-sea communities and oceanographic conditions (Hess et al. 2001; Kuhnt et al. 2005; Yao and Hoteit 2018), fish biology (Gaston, Woo, and Hipfner 2003), changes in coral survival (Genin, Lazar, and Brenner 1995), global hydrological cycles (Trenberth and Dai 2007), etc. Interestingly, a major result of our study is the finding that, while the identified alternative states were equally stable dynamically, structural stability, as measured through the probability of feasibility, dropped across time. Therefore, different metrics of community structure and dynamics should be taken into account for characterizing the ecological state of threatened ecosystems.

513

With more than one million birds wintering in some years, the study area is one of the most important wintering and stopover sites for migratory waterbirds in the Western Palaearctic, supporting more wintering waterfowl than any other site (Marín and García 2006; Rendón et al. 2008; Green et al. 2017; Camacho et al. 2022). The wintering conditions in this region are linked to the survival and breeding output in the breeding headquarters of many waterfowl species in the Western Palaearctic (Rendón et al. 2008; Almaraz et al. 2012; Green et al. 2017; Fox et al. 2023). Interestingly, Ganter and Boyd 2000 presented qualitative evidence of an arctic-wide decline in breeding performance of waterbirds in the summer following the Mt. Pinatubo eruption, with

523 potentially negative effects on wintering waterfowl populations in Southern Europe.
524 This large-scale breeding failure in 1992 was confirmed by local studies with Eurasian
525 Wigeons in Denmark and the UK (Mitchell et al. 2008), and by a reduced hunting bag of
526 several waterfowl species in Denmark from 1982 to 2010 (Christensen and Fox 2014).
527 Given the global relevance of Doñana marshes, it is very likely that the abrupt regime
528 shift detected in 1992 was due to a combination of two factors: 1) a generalized failure
529 of breeding success in the breeding grounds (Ganter and Boyd 2000; Mitchell et al. 2008;
530 Christensen and Fox 2014); and 2) particularly harsh (cold and dry) conditions in the
531 study area during the 1992 winter, compared to other continental wintering grounds
532 (Fig. 2). As shown by the wavelet analysis of precipitation in the study area (Fig. 1),
533 these conditions persisted until 1995. While the evidence suggests that most European
534 waterfowl populations recovered rapidly from the 1992 breeding failure (Ganter and
535 Boyd 2000; Mitchell et al. 2008; Christensen and Fox 2014), it is intriguing that the
536 wintering population in Doñana entered an alternative stable state of significantly lower
537 community abundance, even though local conditions returned to their normal statistical
538 behavior. Although the stochastic cusp catastrophe model we use is a phenomenological
539 approach (Casti 1979; Poston and Stewart 1979), we suggest a biological mechanism ex-
540 plaining the regime shift to an alternative stable state induced by behavioural plasticity.

541
542 Studies on waterfowl migration point to stronger breeding philopatry compared
543 to site fidelity to wintering grounds in these taxa (e.g., Guillemain, Sadoul, and Simon
544 2005; Davis et al. 2014; Clausen and Madsen 2016; Clausen et al. 2018). While geese
545 and swans have been traditionally regarded as bearing stronger fidelity to wintering
546 grounds relative to dabbling ducks and pochards (Robertson and Cooke 1999; Coulson
547 2016), recent data suggest that geese are indeed plastic and can shift flyways with a high
548 probability, even at the individual level (Clausen and Madsen 2016; Clausen et al. 2018;
549 Fox et al. 2023). Pink-footed geese wintering in Denmark, the Netherlands and Belgium,
550 show an average 54% probability of changing migrating strategy during a 25 year
551 period (Clausen et al. 2018). At a continental scale, changes in migration propensity
552 and shifts in flyways and wintering sites are common responses of European ducks to
553 cold or warm spells (Ridgill and Fox 1990; Adam et al. 2015). Abmigration, the ability to
554 shift flyways depending on environmental conditions, is indeed a common strategy in
555 waterfowl: ringing data support the hypothesis that breeding populations of Palaearctic
556 Common Teal can readily shift between North-Western European and Mediterranean
557 flyway routes (Guillemain, Sadoul, and Simon 2005; Parejo et al. 2015). Importantly, site
558 fidelity is usually female-biased in waterfowl and, contrary to other taxa, pair formation
559 may occur in wintering grounds (Robertson and Cooke 1999). As a behavioral strategy
560 under such a strong selective pressure, plasticity in migratory behaviour and wintering
561 grounds in response to rapidly changing environments is thus regarded as adaptive in

562 waterfowl (Clausen and Madsen 2016; Clausen et al. 2018). We suggest that the abrupt
563 regime shift detected in Doñana marshes, followed by an alternative stable state, may
564 be a consequence of a permanent shift to alternative wintering grounds prompted by
565 a perturbation-induced behavioral shift in philopatry. The reversed synoptic climatic
566 conditions uncovered here during the transient Mt. Pinatubo perturbation (Fig. 2)
567 point to an increase in quality for wintering conditions of alternative wintering grounds.
568 These alternative sites may include new reservoirs in Spain (Navedo et al. 2012), and
569 sites in eastern Spain and North Africa where wintering numbers have increased (Kleijn
570 et al. 2014; de Arruda Almeida et al. 2019). Once waterfowl populations undergo a shift
571 in site use in response to local changes in environmental conditions, they may become
572 faithful to these new sites, even after the conditions in the original site improve (Clausen
573 and Madsen 2016; Clausen et al. 2018). This is the behavioural mechanism giving rise to
574 hysteresis (see below). Indeed, even though Doñana Marshes are considered the main
575 wintering site for graylag goose in the Western Palaearctic, the negative shift detected
576 in 1995 has not been reversed, and strong population increases have been observed in
577 northern Spain and several European wintering sites from the mid nineties onwards
578 (Madsen, Cracknell, and Fox 1999; Ramo et al. 2015). In particular, the Danish breeding
579 population of Greylag goose is known to have largely abandoned Doñana marshes as a
580 main wintering sites during the last two decades (Clausen, Heldbjerg, and Fox 2023).
581 Our study covers up to 2013, and future research should assess whether the state in the
582 community adopted from 1996 has remained stable in recent years, especially given
583 the ongoing escalation in global warming. Since 2020, extreme drought and lack of
584 flooded area in the natural marshes has led to exceptionally low numbers of wintering
585 waterfowl (Camacho et al. 2022; Fox et al. 2023). It remains to be seen whether this will
586 lead to a change to a new stable state.

587

588 Recently, theoretical and empirical approaches are addressing the study of nonlinear
589 population dynamics in social species driven by behavioral rapid shifts in response to
590 perturbations, social feedbacks and tipping points (Oro 2020; Oro et al. 2023). According
591 to this perspective, changes in social behaviour induced by disturbances in breeding or
592 wintering grounds may feedback at the population level to induce a highly non-linear
593 dynamics, i.e., a population crash triggered by breeding site abandonment in response
594 to predation (Almaraz and Oro 2011; Oro et al. 2023). In the case of Doñana marshes, we
595 hypothesize that the regime shift to an alternative stable state induced by the transient,
596 large scale climatic perturbation of the Mt. Pinatubo eruption, might be a remarkable
597 example of non-linear feedbacks between behaviour and population dynamics: under
598 this scenario, a persistent reversal of the synoptic climatic fields, with cold and dry
599 conditions in the wintering area, might trigger a trans-generational plastic behavioral
600 shift in migrating birds that persist even under the reversal of the normal synoptic

601 conditions. In this conditions, wintering birds might remain in alternative wintering
602 grounds even if the local conditions return to normal. This might be the mechanism
603 giving rise to hysteresis, as evidenced here in the cusp catastrophe model (Fig. 8).

604

605 Management implications of transients and multi-stability

606 In a rapidly changing world ecological dynamics over short time-scales, at which
607 transient (non-asymptotic) dynamics may govern persistence, arise as a research area
608 of paramount importance from pure and applied standpoints (Hastings et al. 2018).
609 Processes operating with diverging spatial and temporal rates of change may yield
610 surprises if tipping points, bifurcations and alternative stable states are not correctly
611 identified (Watts et al. 2020; Williams, Ordonez, and Svenning 2021; Scheffer 2009).
612 These fundamental scales may have an overriding effect on ecosystem supplies and
613 resilience (Folke et al. 2004; Scheffer 2009). Predicting the consequences of transient
614 environmental dynamics on biological systems is thus essential in global change ecology,
615 with benefits ranging from improved knowledge on ecosystem functioning to informed
616 management of harvested populations (Suding, Gross, and Houseman 2004; Scheffer
617 2009; Francis et al. 2021). A major finding of our study is the decoupling of dynamical
618 stability and structural stability at decadal time scales. We show how feasibility emerges
619 as a key metric to evaluate the extinction risk of threatened communities in biodiver-
620 sity hotspots at risk: while traditional measures of dynamical stability focuses on the
621 asymptotic behaviour of systems, characterizing the changing feasibility domain of
622 threatened communities might inform on the shifts in the structural fragility of already
623 impacted ecosystems. The finding of hysteresis in the wintering waterfowl community
624 of Doñana wetlands and a general decrease of feasibility, brought about by an increase
625 in the probability of species extinction across decades, provides a clear conservation
626 message: when evaluating the current conservation status of threatened ecosystems it
627 is of paramount importance to untangle the detailed history of impacts that drove the
628 system to its current status. In the case of Doñana wetlands, the history uncovered by
629 the present work places in a novel context the already serious threats to the study area
630 (Scheffer et al. 2015; Camacho et al. 2022; Felipe, Aragón, and Díaz-Paniagua 2023;
631 Santamaría and Martín-Ortega 2023).

632

633 Acknowledgements

634 The comments from two anonymous reviewers greatly improved a previous version of
635 the manuscript. PA was supported by a pre-doctoral fellowship through the program

636 Formacion del Profesorado Universitario FPU of the Spanish Ministry of Education
637 (FPU16/00626), and by Proyectos FEDER and Consejería de Economía, Conocimiento,
638 Empresas y Universidad de la Junta de Andalucía, by Programa Operativo FEDER 2014-
639 2020 reference P20-00592. AJG was supported by Ministerio de Ciencia e Innovación.
640 Proyectos de I+D+i PID2020-112774GB-I00 / AEI / 10.13039/501100011033. Census
641 data were collected by the Monitoring Team for Natural Resources and Processes of the
642 EBD-CSIC, and support was provided by the ICTS-RBD.

643

644 Data and code availability

645 All data and reproducible code is available in GitHub <https://github.com/palmaraz/>
646 GuadaluShiftR and Zenodo <https://zenodo.org/records>.

647

648 References

- 649 Adam, Matyáš, Zuzana Musilová, Petr Musil, Jan Zouhar, and Dušan Romportl. 2015.
650 Long-Term Changes in Habitat Selection of Wintering Waterbirds: High Importance
651 of Cold Weather Refuge Sites. *Acta Ornithologica* 50 (2): 127–138. <https://doi.org/10.3161/00016454AO2015.50.2.001>.
- 653 Almaraz, Pablo, Andy J. Green, Eduardo Aguilera, Miguel A. Rendón, and Javier
654 Bustamante. 2012. Estimating partial observability and nonlinear climate effects on
655 stochastic community dynamics of migratory waterfowl. *Journal of Animal Ecology*
656 81 (5): 1113–1125. <https://doi.org/10.1111/j.1365-2656.2012.01972.x>.
- 657 Almaraz, Pablo, José A. Langa, Piotr Kalita, and Fernando Soler-Toscano. 2023. Struc-
658 tural stability of invasion graphs for generalized Lotka-Volterra systems. *arXiv*
659 2209.09802:1–28. <https://doi.org/http://arxiv.org/abs/2209.09802>.
- 660 Almaraz, Pablo, and Daniel Oro. 2011. Size-mediated non-trophic interactions and
661 stochastic predation drive assembly and dynamics in a seabird community. *Ecology*
662 92 (10): 1948–1958. <https://doi.org/10.1890/11-0181.1>.
- 663 Arnoldi, Jean-François, M. Loreau, and B. Haegeman. 2016. Resilience, reactivity and
664 variability: A mathematical comparison of ecological stability measures. *Journal of*
665 *Theoretical Biology* 389:47–59. <https://doi.org/10.1016/j.jtbi.2015.10.012>.

- 666 Barnosky, Anthony D, Elizabeth A Hadly, Jordi Bascompte, Eric L. Berlow, James
667 H. Brown, Mikael Fortelius, Wayne M Getz, John Harte, Alan Hastings, Pablo A
668 Marquet, et al. 2012. Approaching a state shift in Earth's biosphere. *Nature* 486
669 (7401): 52–58. <https://doi.org/10.1038/nature11018>.
- 670 Bjornstad, Ottar N. 2001. Noisy Clockwork: Time Series Analysis of Population Fluctua-
671 tions in Animals. *Science* 293 (5530): 638–643. <https://doi.org/10.1126/science.1062226>.
- 673 Booth, Ben B B, Nick J. Dunstone, Paul R. Halloran, Timothy Andrews, and Nicolas
674 Bellouin. 2012. Aerosols implicated as a prime driver of twentieth-century North
675 Atlantic climate variability. *Nature* 484 (7393): 228–232. <https://doi.org/10.1038/nature10946>.
- 677 Cabon, Antoine, and William R L Anderegg. 2022. Large volcanic eruptions elucidate
678 physiological controls of tree growth and photosynthesis. *Ecology Letters* 26 (2):
679 257–267. <https://doi.org/10.1111/ele.14149>.
- 680 Camacho, Carlos, Juan J. Negro, Johan Elmberg, Anthony D. Fox, Szabolcs Nagy,
681 Deborah J. Pain, and Andy J. Green. 2022. Groundwater extraction poses extreme
682 threat to Doñana World Heritage Site. *Nature Ecology & Evolution*, 2–3. <https://doi.org/10.1038/s41559-022-01763-6>.
- 684 Capon, Samantha J., A. Jasmyn J. Lynch, Nick Bond, Bruce C. Chessman, Jenny Davis,
685 Nick Davidson, Max Finlayson, et al. 2015. Regime shifts, thresholds and multiple
686 stable states in freshwater ecosystems; a critical appraisal of the evidence. *Science of
687 the Total Environment* 534:122–130. <https://doi.org/10.1016/j.scitotenv.2015.02.045>.
- 688 Carpenter, Bob, Andrew Gelman, Matthew D. Hoffman, Daniel Lee, Ben Goodrich,
689 Michael Betancourt, Marcus Brubaker, Jiqiang Guo, Peter Li, and Allen Riddell.
690 2017. Stan : A Probabilistic Programming Language. *Journal of Statistical Software* 76
691 (1). <https://doi.org/10.18637/jss.v076.i01>.
- 692 Casti, J. 1979. Connectivity, Complexity, and Catastrophe in Large-Scale Systems. New
693 York, NY: John Wiley & Sons, Inc.
- 694 ———. 1982. Catastrophes, control and the inevitability of spruce budworm outbreaks.
695 *Ecological Modelling* 14 (3-4): 293–300. [https://doi.org/10.1016/0304-3800\(82\)90024-2](https://doi.org/10.1016/0304-3800(82)90024-2).
- 697 Cazelles, Bernard, Mario Chavez, Dominique Berteaux, Frédéric Ménard, Jon Olav Vik,
698 Stéphanie Jenouvrier, and Nils C. Stenseth. 2008. Wavelet analysis of ecological
699 time series. *Oecologia* 156 (2): 287–304. <https://doi.org/10.1007/s00442-008-0993-2>.

- 700 Chen, Ning, Kailiang Yu, Rongliang Jia, Jialing Teng, and Changming Zhao. 2020.
701 Biocrust as one of multiple stable states in global drylands. *Science Advances* 6 (39):
702 eaay3763. <https://doi.org/10.1126/sciadv.aay3763>.
- 703 Chen, Zhong-Qiang, David A.T. Harper, Stephen Grasby, and Lei Zhang. 2022. Catastrophic event sequences across the Permian-Triassic boundary in the ocean and on
704 land. *Global and Planetary Change* 215:103890. <https://doi.org/10.1016/j.gloplacha.2022.103890>.
- 705 706
- 707 Christensen, Thomas K., and Anthony D. Fox. 2014. Changes in age and sex ratios
708 amongst samples of hunter-shot wings from common duck species in Denmark
709 1982–2010. *European Journal of Wildlife Research* 60 (2): 303–312. <https://doi.org/10.1007/s10344-013-0787-7>.
- 710
- 711 Church, John A., Neil J. White, and Julie M. Arblaster. 2005. Significant decadal-scale
712 impact of volcanic eruptions on sea level and ocean heat content. *Nature* 438 (7064):
713 74–77. <https://doi.org/10.1038/nature04237>.
- 714 Clausen, Kevin K., Henning Heldbjerg, and Anthony D. Fox. 2023. Status, origin and
715 harvest of increasing numbers of Greylag Geese *Anser anser* occurring in Denmark
716 throughout the annual cycle. *Wildfowl* 73:3–25.
- 717 Clausen, Kevin K., and Jesper Madsen. 2016. Philopatry in a changing world: response
718 of pink-footed geese *Anser brachyrhynchus* to the loss of a key autumn staging area
719 due to restoration of Filsø Lake, Denmark. *Journal of Ornithology* 157 (1): 229–237.
720 <https://doi.org/10.1007/s10336-015-1271-9>.
- 721 Clausen, Kevin K., Jesper Madsen, Fred Cottaar, Eckhart Kuijken, and Christine Ver-
722 scheure. 2018. Highly dynamic wintering strategies in migratory geese: Coping
723 with environmental change. *Global Change Biology* 24 (7): 3214–3225. <https://doi.org/10.1111/gcb.14061>.
- 724
- 725 Clements, Christopher F., and Arpat Ozgul. 2018. Indicators of transitions in biological
726 systems. Edited by Jessica Metcalf. *Ecology Letters* 21 (6): 905–919. <https://doi.org/10.1111/ele.12948>.
- 727
- 728 Cobb, Loren, and Shelemyahu Zacks. 1985. Applications of Catastrophe Theory for
729 Statistical Modeling in the Biosciences. *Journal of the American Statistical Association*
730 80 (392): 793–802. <https://doi.org/10.1080/01621459.1985.10478184>.

- 731 Constantinescu, Robert, Aurelian Hopulele-Gligor, Charles B. Connor, Costanza Bonadonna,
732 Laura J. Connor, Jan M. Lindsay, Sylvain Charbonnier, and Alain C. M. Volentik.
733 2021. The radius of the umbrella cloud helps characterize large explosive volcanic
734 eruptions. *Communications Earth & Environment* 2 (1): 3. <https://doi.org/10.1038/s43247-020-00078-3>.
- 735
- 736 Coulson, John C. 2016. A Review of Philopatry in Seabirds and Comparisons with Other
737 Waterbird Species. *Waterbirds* 39 (3): 229–240. <https://doi.org/10.1675/063.039.0302>.
- 738
- 739 Crisafulli, Charles M., Frederick J. Swanson, Jonathan J. Halvorson, and Bruce D. Clark-
740 son. 2015. “Volcano Ecology: Disturbance Characteristics and Assembly of Biologi-
741 cal Communities.” In *The Encyclopedia of Volcanoes*, Second Edi, 1265–1284. Elsevier.
742 <https://doi.org/10.1016/B978-0-12-385938-9.00073-0>.
- 743
- 744 Crosweller, Helen Sian, Baneet Arora, Sarah Krystyna Brown, Elizabeth Cottrell, Natalia
745 Irma Deligne, Natalie Ortiz Guerrero, Laura Hobbs, et al. 2012. Global database
746 on large magnitude explosive volcanic eruptions (LaMEVE). *Journal of Applied
Volcanology* 1 (1): 4. <https://doi.org/10.1186/2191-5040-1-4>.
- 747
- 748 Dakos, Vasilis, Blake Matthews, Andrew P Hendry, Jonathan Levine, Nicolas Loeuille,
749 Jon Norberg, Patrik Nosil, Marten Scheffer, and Luc De Meester. 2019. Ecosystem
750 tipping points in an evolving world. *Nature Ecology & Evolution* 3 (3): 355–362.
<https://doi.org/10.1038/s41559-019-0797-2>.
- 751
- 752 Davis, J. Brian, Matthieu Guillemain, Richard M. Kaminski, Celine Arzel, John M. Eadie,
753 and Eileen C. Rees. 2014. Habitat and resource use by waterfowl in the northern
hemisphere in autumn and winter. *Wildfowl* 4:17–69.
- 754
- 755 de Arruda Almeida, Bia, Esther Sebastián-González, Luiz dos Anjos, Andy J. Green,
756 and Francisco Botella. 2019. A functional perspective for breeding and wintering
waterbird communities: temporal trends in species and trait diversity. *Oikos*, no.
757 February, 1103–1115. <https://doi.org/10.1111/oik.05903>.
- 758
- 759 Denwood, Matthew J. 2016. runjags : An R Package Providing Interface Utilities, Model
760 Templates, Parallel Computing Methods and Additional Distributions for MCMC
761 Models in JAGS. *Journal of Statistical Software* 71 (9). <https://doi.org/10.18637/jss.v071.i09>.
- 762
- 763 Douglass, David H., and Robert S. Knox. 2005. Climate forcing by the volcanic eruption
764 of Mount Pinatubo. *Geophysical Research Letters* 32 (5): 1–5. <https://doi.org/10.1029/2004GL022119>.

- 765 Durant, Joël M., Tycho Anker-Nilssen, Dag O. Hjermann, and Nils Chr Stenseth. 2004.
766 Regime shifts in the breeding of an Atlantic puffin population. *Ecology Letters* 7 (5):
767 388–394. <https://doi.org/10.1111/j.1461-0248.2004.00588.x>.
- 768 Eilers, Paul H. C., and Brian D. Marx. 1996. Flexible smoothing with B-splines and
769 penalties. *Statistical Science* 11 (2): 89–102. <https://doi.org/10.1214/ss/1038425655>.
- 770 Elaydi, Saber N. 2005. An Introduction to Difference Equations. Berlin, Heidelberg:
771 Springer.
- 772 Felipe, Miguel de, David Aragonés, and Carmen Díaz-Paniagua. 2023. Thirty-four years
773 of Landsat monitoring reveal long-term effects of groundwater abstractions on a
774 World Heritage Site wetland. *Science of The Total Environment* 880 (April): 163329.
775 <https://doi.org/10.1016/j.scitotenv.2023.163329>.
- 776 Fernández-Marín, Xavier. 2016. ggmcmc : Analysis of MCMC Samples and Bayesian
777 Inference. *Journal of Statistical Software* 70 (9). <https://doi.org/10.18637/jss.v070.i09>.
- 778 Folke, Carl, Steve Carpenter, Brian Walker, Marten Scheffer, Thomas Elmqvist, Lance
779 Gunderson, and C.S. Holling. 2004. Regime Shifts, Resilience, and Biodiversity in
780 Ecosystem Management. *Annual Review of Ecology, Evolution, and Systematics* 35 (1):
781 557–581. <https://doi.org/10.1146/annurev.ecolsys.35.021103.105711>.
- 782 Fox, Anthony David, Henning Heldbjerg, Kevin Kuhlmann Clausen, Ole Roland Therk-
783 ildsen, Qingshan Zhao, Juan J. Negro, and Andy J. Green. 2023. Danish Greylag
784 Goose *Anser anser* use of the Coto Doñana sand dunes for gritting. *Wildfowl* 73:26–
785 42.
- 786 Francis, Tessa B., Karen C. Abbott, Kim Cuddington, Gabriel Gellner, Alan Hastings,
787 Ying Cheng Lai, Andrew Morozov, Sergei Petrovskii, and Mary Lou Zeeman. 2021.
788 Management implications of long transients in ecological systems. *Nature Ecology
789 and Evolution* 5 (3): 285–294. <https://doi.org/10.1038/s41559-020-01365-0>.
- 790 Fraser, Andrew M. 2008. Hidden Markov Models and Dynamical Systems. 145. Society
791 for Industrial / Applied Mathematics. <https://doi.org/10.1137/1.9780898717747>.
- 792 Fukami, Tadashi, and Mifuyu Nakajima. 2011. Community assembly: alternative stable
793 states or alternative transient states? *Ecology Letters* 14 (10): 973–984. <https://doi.org/10.1111/j.1461-0248.2011.01663.x>.
- 795 Ganter, B., and H. Boyd. 2000. A tropical volcano, high predation pressure, and the
796 breeding biology of Arctic waterbirds: A circumpolar review of breeding failure in
797 the summer of 1992. *Arctic* 53 (3): 289–305. <https://doi.org/10.14430/arctic859>.

- 798 Gaston, Anthony J, Kerry Woo, and J Mark Hipfner. 2003. Trends in Forage Fish Pop-
799 ulations in Northern Hudson Bay since 1981, as Determined from the Diet of
800 Nestling Thick-billed Murres, *< i>Uria lomvia</i>*. *Arctic* 56 (3): 227–233. <https://doi.org/10.14430/arctic618>.
- 802 Genin, Amatzia, Boaz Lazar, and Stephen Brenner. 1995. Vertical mixing and coral death
803 in the red sea following the eruption of Mount Pinatubo. *Nature* 377 (6549): 507–510.
804 <https://doi.org/10.1038/377507a0>.
- 805 Grasman, Raoul P. P. P., Han L. J. van der Maas, and Eric-Jan Wagenmakers. 2009. Fitting
806 the Cusp Catastrophe in R : A cusp Package Primer. *Journal of Statistical Software* 32
807 (8). <https://doi.org/10.18637/jss.v032.i08>.
- 808 Green, Andy J., Paloma Alcorlo, Edwin T.H.M. Peeters, Edward P. Morris, José L.
809 Espinar, Miguel Angel Bravo-Utrera, Javier Bustamante, et al. 2017. Creating a safe
810 operating space for wetlands in a changing climate. *Frontiers in Ecology and the*
811 *Environment* 15 (2): 99–107. <https://doi.org/10.1002/fee.1459>.
- 812 Green, Andy J., Javier Bustamante, Guyonne F. E. Janss, Rocio Fernández-Zamudio, and
813 Carmen Díaz-Paniagua. 2018. “Doñana Wetlands (Spain).” In *The Wetland Book: II:*
814 *Distribution, Description, and Conservation*, edited by C. Max Finlayson, G. Randy Mil-
815 ton, R. Crawford Prentice, and Nick C. Davidson, 1123–1136. Dordrecht: Springer
816 Netherlands.
- 817 Green, Andy J., and Johan Elmberg. 2014. Ecosystem services provided by waterbirds.
818 *Biological Reviews* 89 (1): 105–122. <https://doi.org/10.1111/brv.12045>.
- 819 Green, Theodore, Paul R. Renne, and C. Brenhin Keller. 2022. Continental flood basalts
820 drive Phanerozoic extinctions. *Proceedings of the National Academy of Sciences* 119
821 (38): e20441119. <https://doi.org/10.1073/pnas.2120441119>.
- 822 Gsell, Alena Sonia, Ulrike Scharfenberger, Deniz Özkundakci, Annika Walters, Lars-
823 Anders Hansson, Annette B. G. Janssen, Peeter Nõges, et al. 2016. Evaluating early-
824 warning indicators of critical transitions in natural aquatic ecosystems. *Proceedings*
825 *of the National Academy of Sciences* 113 (50): E8089–E8095. <https://doi.org/10.1073/pnas.1608242113>.
- 827 Gu, Lianhong, Dennis D. Baldocchi, Steve C. Wofsy, J. William Munger, Joseph J. Michal-
828 sky, Shawn P. Urbanski, and Thomas A. Boden. 2003. Response of a deciduous
829 forest to the Mount Pinatubo eruption: Enhanced photosynthesis. *Science* 299 (5615):
830 2035–2038. <https://doi.org/10.1126/science.1078366>.

- 831 Guillemain, M, N Sadoul, and G Simon. 2005. European flyway permeability and
832 abmigration in Teal *Anas crecca*, an analysis based on ringing recoveries. *Ibis* 147
833 (4): 688–696. <https://doi.org/10.1111/j.1474-919X.2005.00446.x>.
- 834 Hansen, James, Andrew Lacis, Reto Ruedy, and Makiko Sato. 1992. Potential climate
835 impact of Mount Pinatubo eruption. *Geophysical Research Letters* 19 (2): 215–218.
836 <https://doi.org/10.1029/91GL02788>.
- 837 Hastings, Alan. 2004. Transients: the key to long-term ecological understanding? *Trends
838 in Ecology & Evolution* 19 (1): 39–45. <https://doi.org/10.1016/j.tree.2003.09.007>.
- 839 Hastings, Alan, Karen C Abbott, Kim Cuddington, Tessa Francis, Gabriel Gellner, Ying-
840 Cheng Lai, Andrew Morozov, Sergei Petrovskii, Katherine Scranton, and Mary
841 Lou Zeeman. 2018. Transient phenomena in ecology. *Science* 361 (6406): eaat6412.
842 <https://doi.org/10.1126/science.aat6412>.
- 843 Hess, Silvia, Wolfgang Kuhnt, Simon Hill, Michael A. Kaminski, Ann Holbourn, and
844 Marietta De Leon. 2001. Monitoring the recolonization of the Mt Pinatubo 1991
845 ash layer by benthic foraminifera. *Marine Micropaleontology* 43 (1-2): 119–142. [https://doi.org/10.1016/S0377-8398\(01\)00025-1](https://doi.org/10.1016/S0377-8398(01)00025-1).
- 847 Hillebrand, Helmut, Ian Donohue, W. Stanley Harpole, Dorothee Hodapp, Michal
848 Kucera, Aleksandra M. Lewandowska, Julian Merder, Jose M. Montoya, and Jan
849 A. Freund. 2020. Thresholds for ecological responses to global change do not
850 emerge from empirical data. *Nature Ecology & Evolution* 4 (11): 1502–1509. <https://doi.org/10.1038/s41559-020-1256-9>.
- 852 Holling, C. S. 1973. Resilience and Stability of Ecological Systems. *Annual Review of
853 Ecology and Systematics* 4:1–23. <https://doi.org/10.1146/annurev.es.04.110173.000245>.
- 855 Jenouvrier, Stéphanie, Henri Weimerskirch, Christophe Barbraud, Young Hyang Park,
856 and Bernard Czelles. 2005. Evidence of a shift in the cyclicity of Antarctic seabird
857 dynamics linked to climate. *Proceedings of the Royal Society B: Biological Sciences* 272
858 (1566): 887–895. <https://doi.org/10.1098/rspb.2004.2978>.
- 859 Jiang, Qiang, Fred Jourdan, Hugo K. H. Olierook, Renaud E. Merle, Julien Bourdet,
860 Denis Fougerouse, Belinda Godel, and Alex T. Walker. 2022. Volume and rate
861 of volcanic CO₂ emissions governed the severity of past environmental crises.
862 *Proceedings of the National Academy of Sciences* 119 (31): e2202039119. <https://doi.org/10.1073/pnas.2202039119>.

- 864 Khodri, Myriam, Takeshi Izumo, Jérôme Vialard, Serge Janicot, Christophe Cassou,
865 Matthieu Lengaigne, Juliette Mignot, et al. 2017. Tropical explosive volcanic eruptions
866 can trigger El Niño by cooling tropical Africa. *Nature Communications* 8 (1):
867 778. <https://doi.org/10.1038/s41467-017-00755-6>.
- 868 Kleijn, David, Imad Cherkaoui, Paul W. Goedhart, Jasper van der Hout, and Dennis
869 Lammertsma. 2014. Waterbirds increase more rapidly in Ramsar-designated wetlands
870 than in unprotected wetlands. Edited by Richard Fuller. *Journal of Applied Ecology* 51 (2): 289–298. <https://doi.org/10.1111/1365-2664.12193>.
- 872 Knowlton, Nancy. 2004. Multiple "stable" states and the conservation of marine ecosystems.
873 *Progress in Oceanography* 60 (2-4): 387–396. <https://doi.org/10.1016/j.pocean.2004.02.011>.
- 875 Knudsen, Mads Faurschou, Bo Holm Jacobsen, Marit-Solveig Seidenkrantz, and Jesper
876 Olsen. 2014. Evidence for external forcing of the Atlantic Multidecadal Oscillation
877 since termination of the Little Ice Age. *Nature Communications* 5 (1): 3323. <https://doi.org/10.1038/ncomms4323>.
- 879 Krakauer, Nir Y., and James T. Randerson. 2003. Do volcanic eruptions enhance or
880 diminish net primary production? Evidence from tree rings. *Global Biogeochemical Cycles* 17 (4): n/a–n/a. <https://doi.org/10.1029/2003GB002076>.
- 882 Kuhnt, Wolfgang, Silvia Hess, Ann Holbourn, Harald Paulsen, and Brigitte Salomon.
883 2005. The impact of the 1991 Mt. Pinatubo eruption on deep-sea foraminiferal communities:
884 A model for the Cretaceous-Tertiary (K/T) boundary? *Palaeogeography, Palaeoclimatology, Palaeoecology* 224 (1-3): 83–107. <https://doi.org/10.1016/j.palaeo.2005.03.042>.
- 887 Kuiper, Jan J., Cassandra van Altena, Peter C. de Ruiter, Luuk P. A. van Gerven, Jan H.
888 Janse, and Wolf M. Mooij. 2015. Food-web stability signals critical transitions in
889 temperate shallow lakes. *Nature Communications* 6 (1): 7727. <https://doi.org/10.1038/ncomms8727>.
- 891 Labitzke, K., and M. P. McCormick. 1992. Stratospheric temperature increases due to
892 Pinatubo aerosols. *Geophysical Research Letters* 19 (2): 207–210. <https://doi.org/10.1029/91GL02940>.
- 894 Loehle, Craig. 1989. Catastrophe theory in ecology: a critical review and an example of
895 the butterfly catastrophe. *Ecological Modelling* 49 (1-2): 125–152. [https://doi.org/10.1016/0304-3800\(89\)90047-1](https://doi.org/10.1016/0304-3800(89)90047-1).
- 897 Logofet, Dmitrii O. 1993. Matrices and Graphs: stability problems in mathematical ecology. 308. Boca Raton, FL: CRC Press.

- 899 Lucht, Wolfgang, I. Colin Prentice, Ranga B. Myneni, Stephen Sitch, Pierre Friedlingstein,
900 Wolfgang Cramer, Philippe Bousquet, Wolfgang Buermann, and Benjamin Smith.
901 2002. Climatic control of the high-latitude vegetation greening trend and Pinatubo
902 effect. *Science* 296 (5573): 1687–1689. <https://doi.org/10.1126/science.1071828>.
- 903 Madsen, Jesper, Gill Cracknell, and Tony Fox. 1999. Goose Populations of the Western
904 Palearctic: A Review of Status and Distribution. Wageningen: Wetlands Interna-
905 tional & NERI.
- 906 Makowski, Dominique, Mattan Ben-Shachar, and Daniel Lüdecke. 2019. bayestestR:
907 Describing Effects and their Uncertainty, Existence and Significance within the
908 Bayesian Framework. *Journal of Open Source Software* 4 (40): 1541. <https://doi.org/10.21105/joss.01541>.
- 910 Marín, C., and F. García. 2006. Doñana, Water and Biosphere. Madrid: Confederación
911 Hidrográfica del Guadalquivir, Ministerio de Medio Ambiente, UNESCO-MaB &
912 Junta de Andalucía.
- 913 May, Robert M. 1977. Thresholds and breakpoints in ecosystems with a multiplicity of
914 stable states. *Nature* 269 (5628): 471–477. <https://doi.org/10.1038/269471a0>.
- 915 McCormick, M. Patrick, Larry W. Thomason, and Charles R. Trepte. 1995. Atmospheric
916 effects of the Mt Pinatubo eruption. *Nature* 373 (6513): 399–404. <https://doi.org/10.1038/373399a0>.
- 918 Millán, L., M. L. Santee, A. Lambert, N. J. Livesey, F. Werner, M. J. Schwartz, H. C.
919 Pumphrey, et al. 2022. The Hunga Tonga-Hunga Ha'apai Hydration of the Strato-
920 sphere. *Geophysical Research Letters* 49 (13): e2022GL099381. <https://doi.org/10.1029/2022GL099381>.
- 922 Mitchell, Carl, Anthony D. Fox, John Harradine, and Ib Clausager. 2008. Measures of
923 annual breeding success amongst Eurasian Wigeon *Anas penelope*. *Bird Study* 55
924 (1): 43–51. <https://doi.org/10.1080/00063650809461503>.
- 925 Montoya, José M., Ian Donohue, and Stuart L. Pimm. 2018. Planetary Boundaries for
926 Biodiversity: Implausible Science, Pernicious Policies. *Trends in Ecology & Evolution*
927 33 (2): 71–73. <https://doi.org/10.1016/j.tree.2017.10.004>.
- 928 Mutshinda, Crispin M., Robert B O'Hara, and Ian P Woiwod. 2009. What drives com-
929 munity dynamics? *Proceedings of the Royal Society B: Biological Sciences* 276 (1669):
930 2923–2929. <https://doi.org/10.1098/rspb.2009.0523>.
- 931 Mutshinda, Crispin M., Robert B. O'Hara, and Ian P. Woiwod. 2011. A multispecies
932 perspective on ecological impacts of climatic forcing. *Journal of Animal Ecology* 80
933 (1): 101–107. <https://doi.org/10.1111/j.1365-2656.2010.01743.x>.

- 934 Nash, Kirsty L., Christopher Cvitanovic, Elizabeth A. Fulton, Benjamin S. Halpern, E. J.
935 Milner-Gulland, Reg A. Watson, and Julia L. Blanchard. 2017. Planetary boundaries
936 for a blue planet. *Nature Ecology & Evolution* 1 (11): 1625–1634. <https://doi.org/10.1038/s41559-017-0319-z>.
- 938 Navedo, J. G., J. A. Masero, J. M. Sánchez-Guzmán, J. M. Abad-Gómez, J. S. Gutiérres,
939 E. G. Sansón, A. Villegas, E. Costillo, C. Corbacho, and R. Morán. 2012. International
940 importance of Extremadura, Spain, for overwintering migratory dabbling ducks: a
941 role for reservoirs. *Bird Conservation International* 22 (3): 316–327. <https://doi.org/10.1017/S0959270911000311>.
- 943 Oppenheimer, Clive. 2003. Climatic, environmental and human consequences of the
944 largest known historic eruption: Tambora volcano (Indonesia) 1815. *Progress in
945 Physical Geography: Earth and Environment* 27 (2): 230–259. <https://doi.org/10.1191/030913303pp379ra>.
- 947 Oro, Daniel. 2020. Perturbation, Behavioural Feedbacks, and Population Dynamics
948 in Social Animals. Oxford University Press. <https://doi.org/10.1093/oso/9780198849834.001.0001>.
- 950 Oro, Daniel, Lluís Alsedà, Alan Hastings, Meritxell Genovart, and Josep Sardanyés. 2023.
951 Social copying drives a tipping point for nonlinear population collapse. *Proceedings
952 of the National Academy of Sciences* 120 (11): e2214055120. <https://doi.org/10.1073/pnas.2214055120>.
- 954 Osipov, Sergey, Georgiy Stenchikov, Kostas Tsigaridis, Allegra N. LeGrande, Susanne E.
955 Bauer, Mohammed Fnais, and Jos Lelieveld. 2021. The Toba supervolcano erup-
956 tion caused severe tropical stratospheric ozone depletion. *Communications Earth &
957 Environment* 2 (1): 71. <https://doi.org/10.1038/s43247-021-00141-7>.
- 958 Osland, Michael J., Laura C. Feher, Gordon H. Anderson, William C. Vervaeke, Ken W.
959 Krauss, Kevin R.T. Whelan, Karen M. Valentine, Ginger Tiling-Range, Thomas J.
960 Smith, and Donald R. Cahoon. 2020. A Tropical Cyclone-Induced Ecological Regime
961 Shift: Mangrove Forest Conversion to Mudflat in Everglades National Park (Florida,
962 USA). *Wetlands* 40 (5): 1445–1458. <https://doi.org/10.1007/s13157-020-01291-8>.
- 963 Otterå, Odd Helge, Mats Bentsen, Helge Drange, and Lingling Suo. 2010. External
964 forcing as a metronome for Atlantic multidecadal variability. *Nature Geoscience* 3
965 (10): 688–694. <https://doi.org/10.1038/ngeo955>.

- 966 Parejo, Manuel, Juan G. Navedo, Jorge S. Gutiérrez, José M. Abad-Gómez, Auxiliadora
967 Villegas, Casimiro Corbacho, Juan M. Sánchez-Guzmán, and José A. Masero. 2015.
968 Geographical origin of dabbling ducks wintering in Iberia: sex differences and
969 implications for pair formation. *Ibis* 157 (3): 536–544. <https://doi.org/10.1111/ibi.12256>.
- 971 Petraitis, Peter. 2013. Multiple Stable States in Natural Ecosystems. Oxford, UK: Oxford
972 University Press. <https://doi.org/10.1093/acprof:osobl/9780199569342.001.0001>.
- 973 Piersma, Theunis, and Jan A. van Gils. 2011. The Flexible Phenotype: A body-centred
974 integration of ecology, physiology, and behaviour. Oxford, UK: Oxford University
975 Press.
- 976 Plummer, Martyn. 2003. JAGS: A program for analysis of Bayesian graphical models
977 using Gibbs sampling. In *Proceedings of the 3rd International Workshop on Distributed*
978 *Statistical Computing*, March, 20–30. <https://doi.org/10.1.1.13.3406>.
- 979 Post, Eric. 2013. Ecology of Climate Change: The Importance of Biotic Interactions.
980 Princeton, NJ.: Princeton University Press.
- 981 Poston, Tim, and Ian Stewart. 1979. Catastrophe Theory and Its Applications. London,
982 UK.: Pitman Publishing.
- 983 Ramo, Cristina, Eduardo Aguilera, Jordi Figuerola, Manuel Máñez, and Andy J. Green.
984 2013. Long-Term Population Trends of Colonial Wading Birds Breeding in Doñana
985 (Sw Spain) in Relation to Environmental and Anthropogenic Factors. *Ardeola* 60 (2):
986 305–326. <https://doi.org/10.13157/arpa.60.2.2013.305>.
- 987 Ramo, Cristina, Juan A. Amat, Leif Nilsson, Vincent Schricke, Mariano Rodríguez-
988 Alonso, Enrique Gómez-Crespo, Fernando Jubete, et al. 2015. Latitudinal-Related
989 Variation in Wintering Population Trends of Greylag Geese (*Anser Anser*) along
990 the Atlantic Flyway: A Response to Climate Change? Edited by Roberto Ambrosini.
991 *PLOS ONE* 10 (10): e0140181. <https://doi.org/10.1371/journal.pone.0140181>.
- 992 Ranta, Esa, Per Lundberg, and Veijo Kaitala. 2006. Ecology of Populations. Cambridge,
993 UK: Cambridge University Press.
- 994 Rees, Charles B. van, David Aragonés, Willem Bouten, Chris B. Thaxter, Eric W. M.
995 Stienen, Javier Bustamante, and Andy J. Green. 2021. Dynamic space use of Andalu-
996 sian rice fields by Lesser Black-backed Gulls (*Larus fuscus*) is driven by flooding
997 pattern. *Ibis* 163 (4): 1252–1270. <https://doi.org/10.1111/ibi.12968>.

- 998 Rendón, M.A., A.J. Green, E. Aguilera, and P. Almaraz. 2008. Status, distribution and
999 long-term changes in the waterbird community wintering in Doñana, south-west
1000 Spain. *Biological Conservation* 141 (5): 1371–1388. <https://doi.org/10.1016/j.biocon.2008.03.006>.
- 1002 Ridgill, S.C., and A.D. Fox. 1990. *Cold weather movements of waterfowl in Western Europe*.
1003 Technical report. Slimbridge, UK.: IWRB Special Publ. 13.
- 1004 Roberts, Alan. 1974. The stability of a feasible random ecosystem. *Nature* 251:607–608.
1005 [https://doi.org/10.1016/0025-5564\(75\)90030-9](https://doi.org/10.1016/0025-5564(75)90030-9).
- 1006 Robertson, Gregory J., and Fred Cooke. 1999. Winter Philopatry in Migratory Waterfowl.
1007 *The Auk* 116 (1): 20–34. <https://doi.org/10.2307/4089450>.
- 1008 Robock, Alan. 2000. Volcanic eruptions and climate. *Reviews of Geophysics* (Dordrecht)
1009 38 (2): 191–219. <https://doi.org/10.1029/1998RG000054>.
- 1010 ———. 2002. The Climatic Aftermath. *Science* 295 (5558): 1242–1244. <https://doi.org/10.1126/science.1069903>.
- 1012 Rocha, Juan C, Garry Peterson, Orjan Bodin, and Simon Levin. 2018. Cascading regime
1013 shifts within and across scales. *Science* 362 (6421): 1379–1383. <https://doi.org/10.1126/science.aat7850>.
- 1015 Rocha, Juan Carlos, Garry D. Peterson, and Reinette Biggs. 2015. Regime shifts in the
1016 anthropocene: Drivers, risks, and resilience. *PLoS ONE* 10 (8): e0134639. <https://doi.org/10.1371/journal.pone.0134639>.
- 1018 Rockström, Johan, Will Steffen, Kevin Noone, Asa Persson, F. Stuart Chapin, Eric F.
1019 Lambin, Timothy M. Lenton, et al. 2009. A safe operating space for humanity.
1020 *Nature* 461 (7263): 472–475. <https://doi.org/10.1038/461472a>.
- 1021 Rudnick, Daniel L., and Russ E. Davis. 2003. Red noise and regime shifts. *Deep-Sea
1022 Research Part I: Oceanographic Research Papers* 50 (6): 691–699. [https://doi.org/10.1016/S0967-0637\(03\)00053-0](https://doi.org/10.1016/S0967-0637(03)00053-0).
- 1024 Sadler, J. P., and J. P. Grattan. 1999. Volcanoes as agents of past environmental change.
1025 *Global and Planetary Change* 21 (1-3): 181–196. [https://doi.org/10.1016/S0921-8181\(99\)00014-4](https://doi.org/10.1016/S0921-8181(99)00014-4).
- 1027 Santamaría, Luis, and Julia Martin-Ortega. 2023. How Europe's most iconic wetland
1028 could be finished off by a strawberry farming bill. *Nature Water* 1 (7): 564–565.
1029 <https://doi.org/10.1038/s44221-023-00100-w>.
- 1030 Scheffer, Marten. 2009. Critical Transitions in Nature and Society. Princeton, NJ.: Prince-
1031 ton University Press.

- 1032 Scheffer, Marten, S. Barrett, S. R. Carpenter, C Folke, A. J. Green, M. Holmgren, T. P.
1033 Hughes, et al. 2015. Creating a safe operating space for iconic ecosystems. *Science*
1034 347 (6228): 1317–1319. <https://doi.org/10.1126/science.aaa3769>.
- 1035 Schoener, Thomas W., and David A. Spiller. 2006. Nonsynchronous recovery of commu-
1036 nity characteristics in island spiders after a catastrophic hurricane. *Proceedings of
1037 the National Academy of Sciences* 103 (7): 2220–2225. [https://doi.org/10.1073/pnas.0510355103](https://doi.org/10.1073/pnas.
1038 0510355103).
- 1039 Sebastián-González, Esther, and Andy J. Green. 2016. Reduction of avian diversity
1040 in created versus natural and restored wetlands. *Ecography* 39 (12): 1176–1184.
1041 <https://doi.org/10.1111/ecog.01736>.
- 1042 Sguotti, Camilla, Saskia A Otto, Romain Frelat, Tom J Langbehn, Marie Plambech
1043 Ryberg, Martin Lindegren, Joël M. Durant, Nils Chr. Stenseth, and Christian Möll-
1044 mann. 2019. Catastrophic dynamics limit Atlantic cod recovery. *Proceedings of the
1045 Royal Society B: Biological Sciences* 286 (1898): 20182877. [https://doi.org/10.1098/rspb.2018.2877](https://doi.org/10.1098/
1046 rspb.2018.2877).
- 1047 Smith, Doug M., Ben B.B. Booth, Nick J. Dunstone, Rosie Eade, Leon Hermanson, Gareth
1048 S. Jones, Adam A. Scaife, Katy L. Sheen, and Vikki Thompson. 2016. Role of volcanic
1049 and anthropogenic aerosols in the recent global surface warming slowdown. *Nature
1050 Climate Change* 6 (10): 936–940. <https://doi.org/10.1038/nclimate3058>.
- 1051 Soden, B J, R T Wetherald, G L Stenchikov, and A Robock. 2002. Global cooling after the
1052 eruption of Mount Pinatubo: a test of climate feedback by water vapour. *Science*
1053 296 (26 April): 727–730. <https://doi.org/10.1126/science.296.5568.727>.
- 1054 Song, Chuliang, and Serguei Saavedra. 2018. Will a small randomly assembled commu-
1055 nity be feasible and stable? *Ecology* 99 (3): 743–751. [https://doi.org/10.1002/ecy.2125](https://doi.org/10.1002/ecy.
1056 2125).
- 1057 Steele, John H. 1996. Regime shifts in fisheries management. *Fisheries Research* 25 (95):
1058 19–23. [https://doi.org/10.1016/0165-7836\(95\)00440-8](https://doi.org/10.1016/0165-7836(95)00440-8).
- 1059 Steffen, Will, Katherine Richardson, Johan Rockström, Sarah E. Cornell, Ingo Fetzer,
1060 Elena M. Bennett, Reinette Biggs, et al. 2015. Planetary boundaries: Guiding human
1061 development on a changing planet. *Science* 347:1259855. [https://doi.org/10.1126/science.1259855](https://doi.org/10.1126/
1062 science.1259855).
- 1063 Stelzer, Julio Alberto Alegre, Jorrit Padric Mesman, Rita Adrian, and Bastiaan Willem
1064 Ibelings. 2021. Early warning signals of regime shifts for aquatic systems: Can
1065 experiments help to bridge the gap between theory and real-world application?
1066 *Ecological Complexity* 47:100944. <https://doi.org/10.1016/j.ecocom.2021.100944>.

- 1067 Suding, Katharine N., Katherine L. Gross, and Gregory R. Houseman. 2004. Alternative
1068 states and positive feedbacks in restoration ecology. *Trends in Ecology & Evolution*
1069 19 (1): 46–53. <https://doi.org/10.1016/j.tree.2003.10.005>.
- 1070 Thom, René. 1975. Structural stability and morphogenesis. Reading, USA: W. A. Ben-
1071 jamin, Inc.
- 1072 ———. 1977. Structural Stability, Catastrophe Theory, and Applied Mathematics. *SIAM*
1073 *Review* 19 (2): 189–201. <https://doi.org/10.1137/1019036>.
- 1074 Torrence, Christopher, and Gilbert P Compo. 1998. A Practical Guide to Wavelet Analy-
1075 sis. *Bulletin of the American Meteorological Society* 79 (1): 61–78.
- 1076 Trenberth, Kevin E., and Aiguo Dai. 2007. Effects of Mount Pinatubo volcanic eruption
1077 on the hydrological cycle as an analog of geoengineering. *Geophysical Research*
1078 *Letters* 34 (15): L15702. <https://doi.org/10.1029/2007GL030524>.
- 1079 Vázquez-Loureiro, David, Vítor Gonçalves, Alberto Sáez, Armand Hernández, Pedro M.
1080 Raposeiro, Santiago Giralt, María J. Rubio-Inglés, Valentí Rull, and Roberto Bao.
1081 2019. Diatom-inferred ecological responses of an oceanic lake system to volcanism
1082 and anthropogenic perturbations since 1290 CE. *Palaeogeography, Palaeoclimatology,*
1083 *Palaeoecology* 534 (July): 109285. <https://doi.org/10.1016/j.palaeo.2019.109285>.
- 1084 Vellend, Mark. 2016. The Theory of Ecological Communities. Princeton, NJ.: Princeton
1085 University Press.
- 1086 Walton, M.E.M., C. Vilas, J.P. Cañavate, E. Gonzalez-Ortegon, A. Prieto, S.A. van Bergeijk,
1087 A.J. Green, M. Librero, N. Mazuelos, and L. Le Vay. 2015. A model for the future:
1088 Ecosystem services provided by the aquaculture activities of Veta la Palma, South-
1089 ern Spain. *Aquaculture* 448:382–390. <https://doi.org/10.1016/j.aquaculture.2015.06.017>.
- 1091 Ward, Eric J., Sean C. Anderson, Mary E. Hunsicker, and Michael A. Litzow. 2022.
1092 Smoothed dynamic factor analysis for identifying trends in multivariate time series.
1093 *Methods in Ecology and Evolution* 13 (4): 908–918. <https://doi.org/10.1111/2041-210X.13788>.
- 1095 Watts, Kevin, Robin C. Whytock, Kirsty J. Park, Elisa Fuentes-Montemayor, Nicholas A.
1096 Macgregor, Simon Duffield, and Philip J. K. McGowan. 2020. Ecological time lags
1097 and the journey towards conservation success. *Nature Ecology & Evolution* 4 (3):
1098 304–311. <https://doi.org/10.1038/s41559-019-1087-8>.

- 1099 Williams, John W., Alejandro Ordonez, and Jens Christian Svenning. 2021. A unifying
1100 framework for studying and managing climate-driven rates of ecological change.
1101 *Nature Ecology and Evolution* 5 (1): 17–26. [https://doi.org/10.1038/s41559-020-01344-5](https://doi.org/10.1038/s41559-020-
1102 01344-5).
- 1103 Yang, Qiang, Mike S. Fowler, Andrew L. Jackson, and Ian Donohue. 2019. The pre-
1104 dictability of ecological stability in a noisy world. *Nature Ecology & Evolution* 3 (2):
1105 251–259. <https://doi.org/10.1038/s41559-018-0794-x>.
- 1106 Yao, Fengchao, and Ibrahim Hoteit. 2018. Rapid Red Sea Deep Water renewals caused
1107 by volcanic eruptions and the North Atlantic Oscillation. *Science Advances* 4 (6):
1108 eaar5637. <https://doi.org/10.1126/sciadv.aar5637>.
- 1109 Yletyinen, Johanna, Orjan Bodin, Benjamin Weigel, Marie C. Nordström, Erik Bonsdorff,
1110 and Thorsten Blenckner. 2016. Regime shifts in marine communities: a complex
1111 systems perspective on food web dynamics. *Proceedings of the Royal Society B:
1112 Biological Sciences* 283 (1825): 20152569. <https://doi.org/10.1098/rspb.2015.2569>.

Tables and figures**List of Tables**

1115 1	Comparison of model fits between a linear model, a logistic model and the cusp catastrophe model	36
-------------	---	----

List of Figures

1118 1	Environmental and stratospheric aerosol optical depth time series	37
1119 2	Synoptic fields of composite anomalies obtained from the V3 of the Twentieth Century Reanalysis Project	38
1120 3	Posterior estimated community common DFA trends	39
1121 4	Posterior estimated common trends of the state-space DFA	40
1122 5	Factors loadings of the state-space DFA	41
1123 6	Posterior distribution of dynamical stability and feasibility in alternative stable states	42
1124 7	Change in probability of species extinction between two periods	43
1125 8	Three-dimensional diagram of the fitted stochastic cusp catastrophe model	44

Table 1: Comparison of model fits between a linear model, a logistic model and the cusp catastrophe model. n_p is the number of parameters; pseudo – R^2 specifies the proportion of variance explained by each model; *logLik* is the minimized log-likelihood function; AIC is the small-sample corrected Akaike Information Criterion, and BIC the Bayesian Information Criterion.

Model	n_p	pseudo – R^2	logLik	AICc	BIC
Linear	4	0.129	-20.678	50.647	55.690
Logistic	4	0.185	-19.504	48.299	53.343
Cusp	6	0.954	-10.426	35.749	42.353

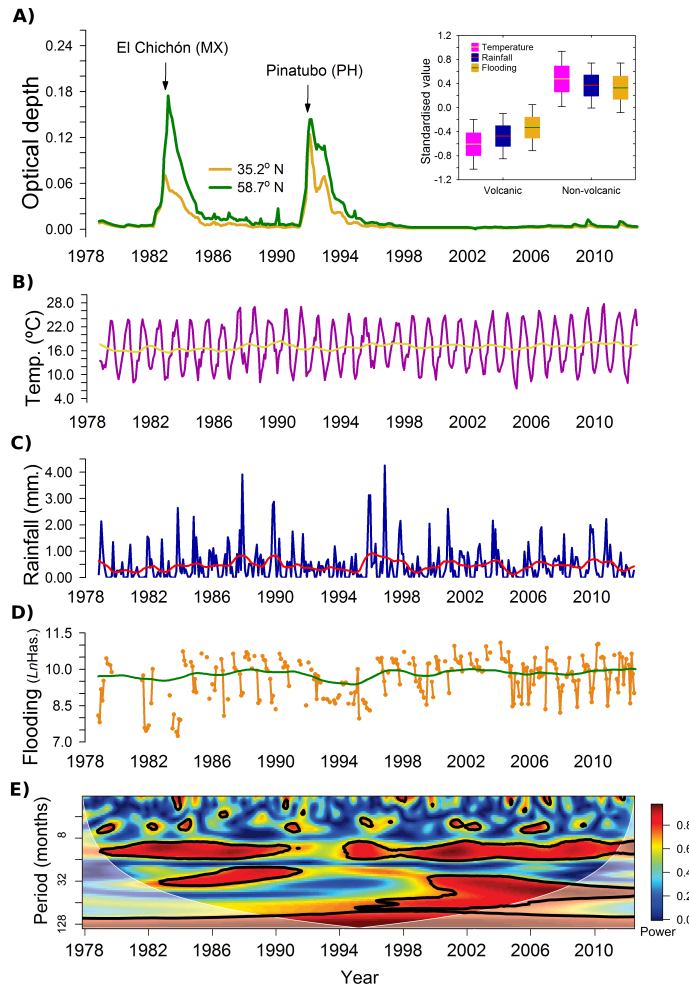


Figure 1: Temporal evolution at monthly steps of the environmental variables used in this study. **A)** Time series for the stratospheric aerosol optical depth (adim.) in the Northern hemisphere, in yellow and green at two different latitudes (Booth et al. 2012). The massive stratospheric aerosol injection events of the two largest volcanic eruptions of the study period, El Chichón (Mexico) and Mt. Pinatubo (Philippines), are located with arrows. The inset figure shows the box-plots for the average (horizontal line within each box), Standard Error (Box size) and Standard Deviation (whiskers) of the standardized variables of temperature, precipitation and spatial flooding extension, during volcanic years (1982-1983 and 1992-1995) and non-volcanic years. **B)** Monthly time series of temperature (°C) in the study area (Almaraz et al. 2012, in purple), with smoothed loess fitting in yellow. **C)** Rainfall (mm.) in the study area in blue, with smoothed loess fitting in red. **D)** Spatial flooding extension ($\ln(\text{Has.})$) in the Doñana wetlands, including all types of flooded surfaces in orange, with smoothed loess fitting in green. **E)** Wavelet spectrum for the precipitation time series (Cazelles et al. 2008). Power values within black contours indicate statistically significant periodicity.

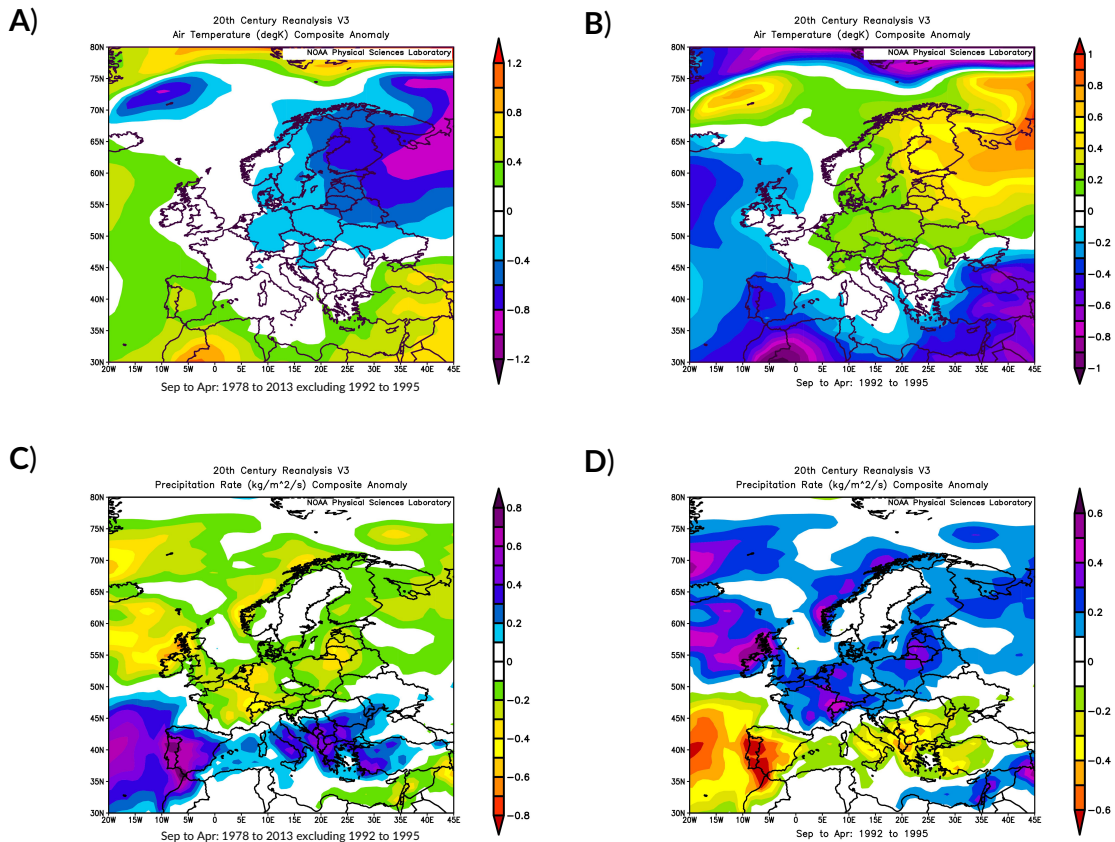


Figure 2: Synoptic fields of composite anomalies obtained from the V3 of the Twentieth Century Reanalysis Project (https://psl.noaa.gov/data/20thC_Rean/). The composite anomaly from 1978 to 2013, excluding the transient period 1992-1995, is shown for air temperature (A) and precipitation rate (C). The composite anomaly for the transient period, 1992-1995, is shown for air temperature (B) and precipitation rate (D). The seasonal period considered excludes the summer months.

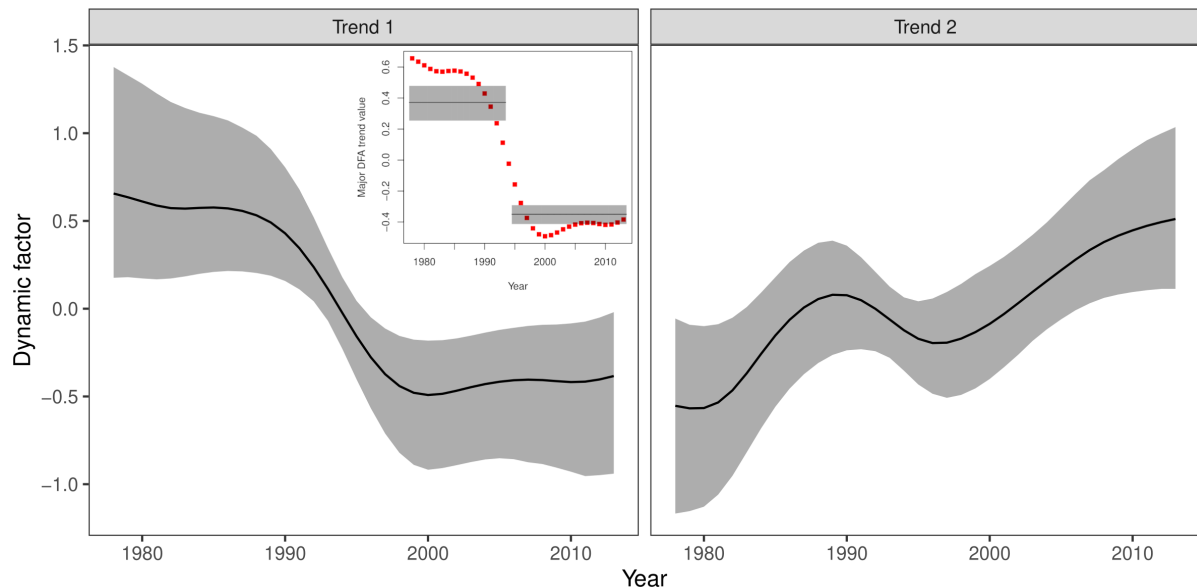


Figure 3: Posterior estimated community common trends in abundance of the state-space Dynamic Factor Analysis (Ward et al. 2022) applied to the wintering waterfowl community, and 95 % credible intervals. The inset figure in the common trend 1 shows the posterior regime shift identified by a Hidden Markov Model applied to the first common trend of the state-space DFA. The values of the common trend are depicted as red axes, and the average (and 95% Credible Intervals) of each regime is denoted in gray.

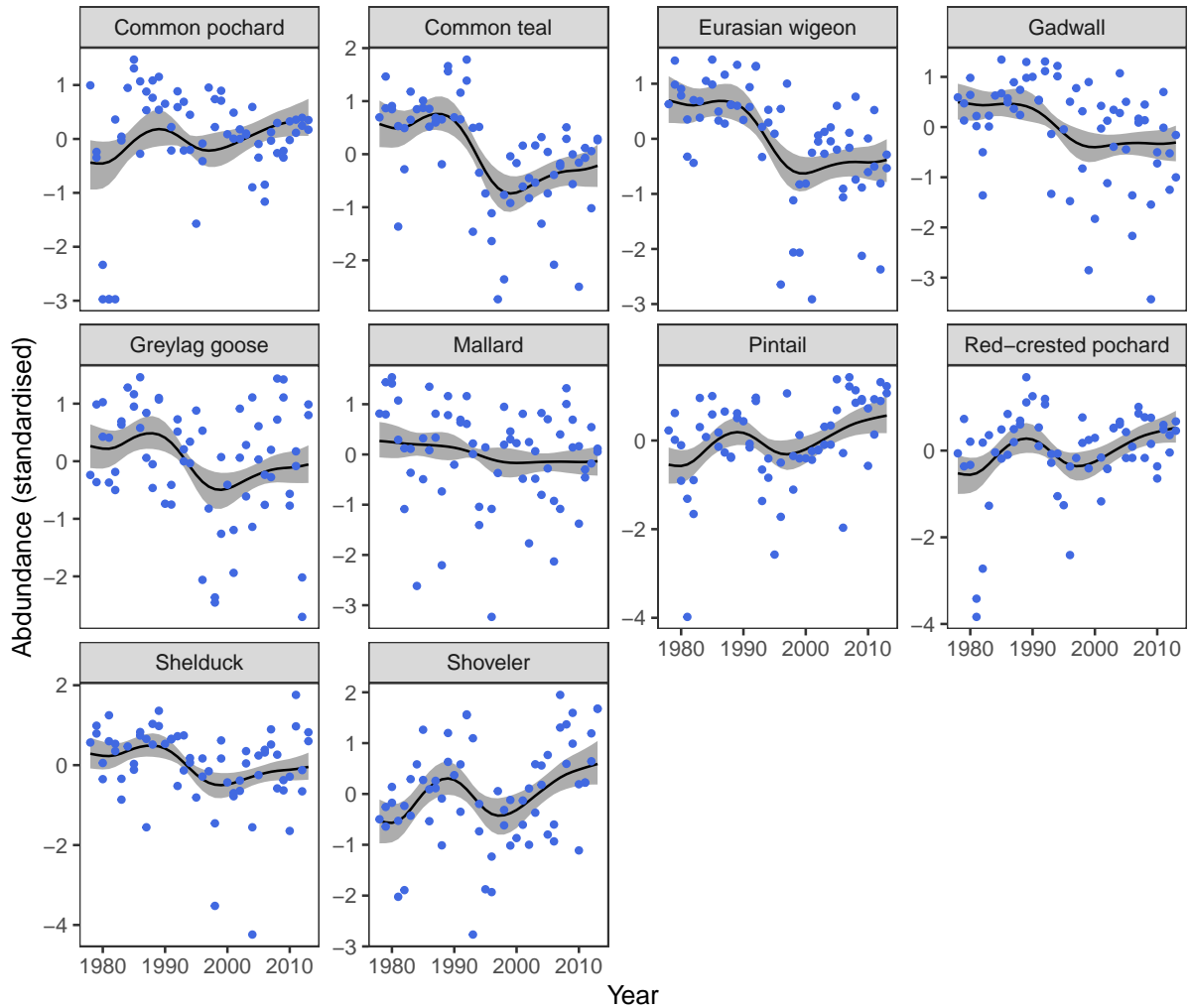


Figure 4: Posterior estimated common trends of the state-space Dynamic Factor Analysis for each wintering waterfowl species in Doñana wetlands, 1978-2021. The red dots denote the aerial count estimate for December and January of each wintering season. The solid line is the average posterior value of the common trend in Figure 3 yielding the largest factor loading for each species (Figure 5), and the shaded region is 95 % credible intervals.

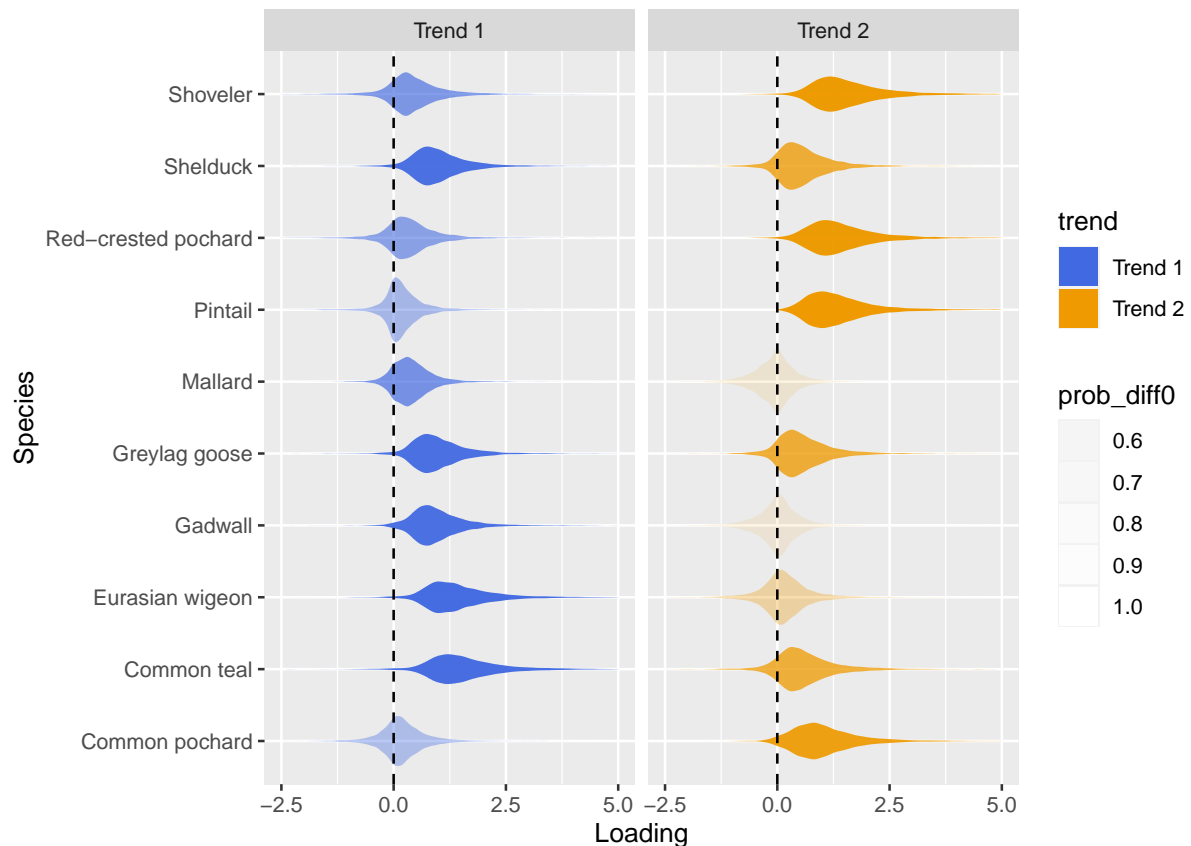


Figure 5: Factors loadings of the state-space Dynamic Factor Analysis for each wintering waterfowl species and each dynamic common trend (shown in Figs. 3 and 4). Violin plots include the posterior density for each loading and species, and the gray shading (prob diff0) is proportional to the probability that the loading is different from 0.

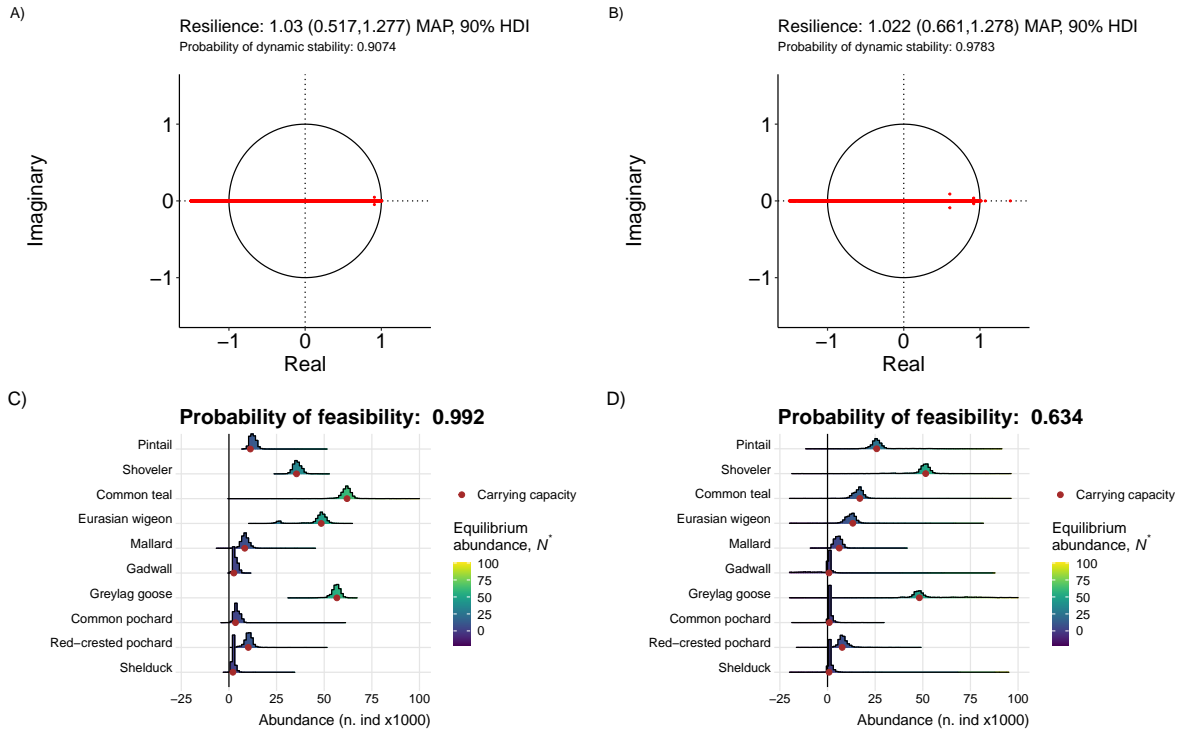


Figure 6: Probability of dynamical stability and feasibility of the wintering waterfowl community in Doñana marshes (1978-2013). Figures A) and B) show the distribution in the unit circle of the posterior eigenvalues of the Jacobian matrix 5 of the LVR state-space model (Eqns. 2-4) fitted to the pre-Pinatubo period (A, 1978-1992) and the post-Pinatubo period (B, 1995-2013). The probability of stability is the fraction of the eigenvalues (modulus) strictly smaller than 1 in the posterior distribution. MAP is the maximum a posteriori density, and 90% HDI the highest density interval (Makowski, Ben-Shachar, and Lüdecke 2019). Figures C) and D) show the posterior histograms of the equilibrium abundances (N^*) and the posterior averages of the carrying capacities, k_i (Eqn. 2), for each waterfowl species (red dots) in the pre-Pinatubo period (C) and the post-Pinatubo period (D). The probability of feasibility for each period is the proportion of posterior estimated equilibrium abundance vectors in which the abundances are strictly positive for all species.

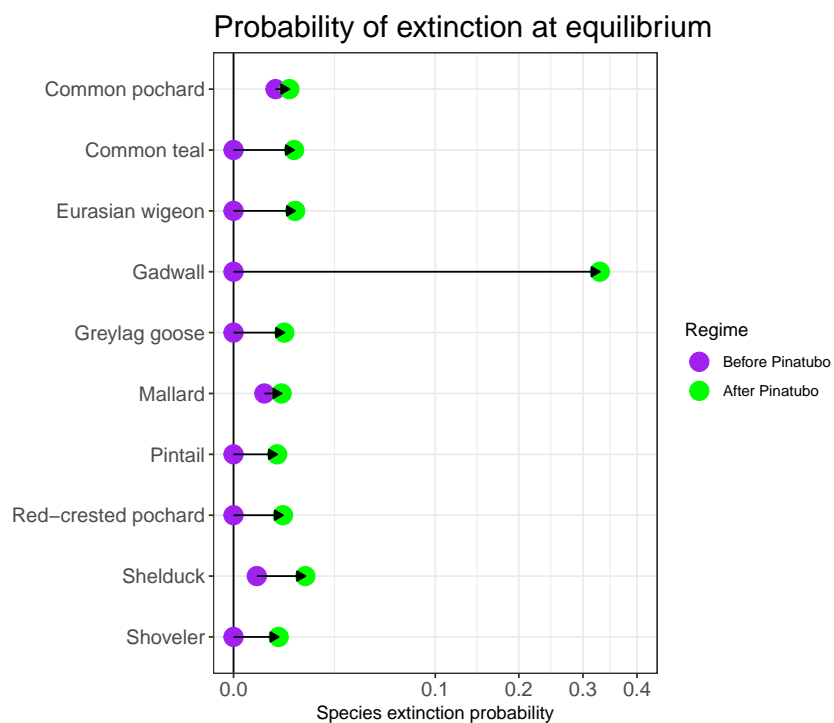


Figure 7: Change in the estimated probability of extinction at equilibrium for each waterfowl species in Doñana wetlands before (purple dots) and after the eruption of Mt. Pinatubo (green dots). From the posterior of the Bayesian regime-dependent state-space LVR model (Eqns. 2-4) fitted to the time-series of community abundance, this probability is calculated, for each species and alternative stable state, as the fraction of posterior estimated population abundances at equilibrium that are not strictly positive. Note the *sqrt*-transformation of the *x*-axis.

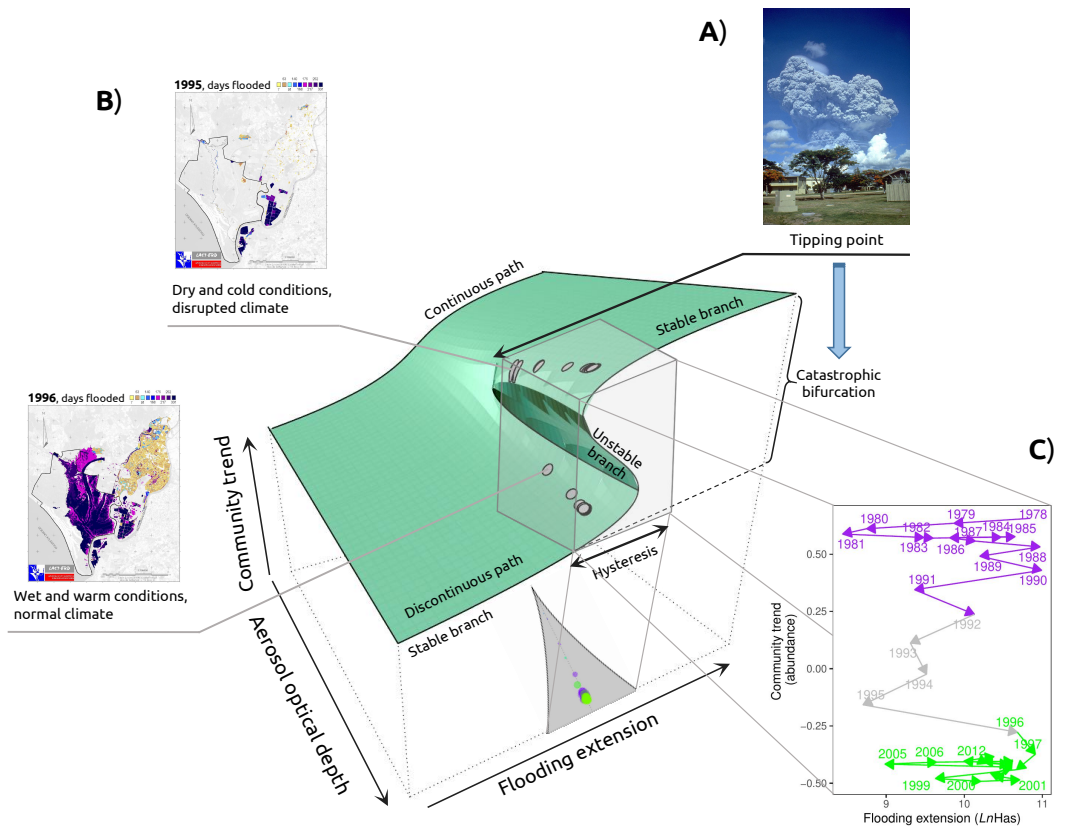


Figure 8: Diagram depicting the three-dimensional representation of the stochastic cusp catastrophe model (Eqn. 6) fitted to the major community trend (z-axis, Trend 1 in Fig. 3), as a function of the stratospheric aerosol optical depth (bifurcation parameter) and flooding extension (asymmetry parameter). The fitted values plotted in the maximum-likelihood cusp equilibrium surface (in green) are depicted as gray circles. In A), the tipping point (the cusp) of the model is represented by the eruption of Mt. Pinatubo of Philippines in April 2, 1991. As a press-type perturbation, it triggered a transient period of dry and cold wintering conditions in the Southern Palaearctic that lasted until 1995 (Robock 2002). Before the tipping point, fluctuations in waterfowl community abundance were located in the upper stable branch of the surface. In B), the small figures show maps of the numbers of days of flooded conditions in Doñana wetlands for two distinct years: 1995, at the end of transient period characterized by dry and cold wintering conditions; and 1996, a climatically normal year, with wet and warm conditions (see Fig. 2). The dynamic in year 1995 was evolving in the unstable (transient) branch of the surface. From 1996 onwards, the dynamics settled in the lower stable branch. The magnitude of the catastrophic bifurcation triggered by the tipping point is thus the difference in height between the two stable branches, while the size of the region of hysteresis is the amplitude of the stable states of waterfowl community abundance sharing the same environmental conditions. The gray cube in B), with height equal to the size of the catastrophic bifurcation, and width equal to the size of the hysteresis region, contains all the dynamics of the system, that takes place along the discontinuous paths. The bifurcation set is projected as a gray shadow in the floor of the cusp 3D surface, with the cusp as a critical point in the vertex. This set is represented in 2-dimensions in C), where the implicit temporal dynamics of the community abundance trend evolves with respect to the asymmetry parameter, namely flooding extension, from the first stable state (purple arrows) to the second stable state (green arrows) through the transient, unstable period (gray arrows). Flooding data provided by the LAST-EBD; Pinatubo public domain image from [Richard P. Hoblitt, USGS](#).